



The CStools (v4.0) Toolbox: from Climate Forecasts to Climate Forecast Information

- Núria Pérez-Zanón¹, Louis-Philippe Caron^{1,2}, Silvia Terzago³, Bert Van Schaeybroeck⁴, Llorenç Lledó¹, Nicolau Manubens¹, Emmanuel Roulin⁴, M. Carmen Alvarez-Castro⁵, Lauriane Batté⁶,
5 Carlos Delgado-Torres¹, Marta Domínguez⁷, Jost von Hardenberg^{8,3}, Eroteida Sánchez-García⁷,
Verónica Torralba¹, Deborah Verfaillie⁹
- ¹Barcelona Supercomputing Center (BSC), Barcelona, Spain
²Ouranos, 550 Sherbrooke St W, Montreal, Quebec H3A9, Canada
³National Research Council of Italy, Institute of Atmospheric Sciences and Climate (CNR-ISAC), Turin, Italy
10 ⁴Royal Meteorological Institute of Belgium, Brussels, Belgium
⁵Fondazione Centro Euro-Mediterraneo sui Cambiamenti Climatici (CMCC), Bologna, Italy
⁶CNRM, Université de Toulouse, Météo-France, CNRS, Toulouse, France
⁷Delegación territorial (DT) Cantabria, Agencia Estatal de Meteorología (AEMET), Santander, Spain
⁸Dept. of Environment, Land and Infrastructure Engineering, Politecnico di Torino, Turin, Italy
15 ⁹Earth and Life Institute, Université catholique de Louvain, Louvain-la-Neuve, Belgium

Correspondence to: Núria Pérez-Zanón (nuria.perez@bsc.es)

- Abstract.** Despite the wealth of existing climate forecast data, only a small part is effectively exploited for sectoral applications. A major cause of this is the lack of integrated tools that allow the translation of data into useful and skilful climate information. This barrier is addressed through the development of an R package. CStools is an easy-to-use toolbox
20 designed and built to assess and improve the quality of climate forecasts for seasonal to multi-annual scales. The package contains process-based state-of-the-art methods for forecast calibration, bias correction, statistical and stochastic downscaling, optimal forecast combination and multivariate verification, as well as basic and advanced tools to obtain tailored products. Due to the design of the toolbox in individual functions, the users can develop their own post-processing chain of functions as shown in the use cases presented in this manuscript: the analysis of an extreme wind speed event, the
25 generation of seasonal forecasts of snow depth based on the SNOWPACK model and the post-processing of data to be used as input for the SCHEME hydrological model.

1 Introduction

1.1 The need for climate information

- Large multi-model seasonal forecasting systems have been developed in recent years, both from current international
30 research projects and operational programmes. These include, for instance, EUROSIP (Vitart et al., 2007; Mishra et al., 2019), APEC (Wang et al., 2009; Min et al., 2014), North-American Multi-Model Ensembles (Kirtman et al., 2014), and the Decadal Climate Prediction Project (CMIP6-DCPP, Boer et al., 2016). More recently, the Copernicus Climate Change Service (C3S) funded by the European Union established a Climate Data Store (CDS) with the aim of being an authoritative source for distributing relevant datasets for a wide range of applications, including an ensemble of (mostly) European
35 Seasonal Forecasting Systems.

- In parallel, there has been an increasing demand for reliable climate information and tailored climate services, in particular at the seasonal timescale, as this period coincides with the planning horizon in several sectors of activities (Troccoli et al., 2008). However, large availability of climate data does not automatically imply stakeholders have access to useful climate
40 information. Indeed, post-processing methods with different levels of sophistication are required to convert climate data into tailored climate information, allowing users and decision-makers to develop and implement strategies of adaptation to



climate variability and to guide well-informed decision making. In fact, there is a strong need and interest in a wide range of application sectors for reliable seasonal to decadal forecasts (White et al., 2017). Moreover, the generation of products adjusted to user needs tends to be costly in time and resources. Software tools facilitate this process, by sharing common and state-of-the-art methods with actors in the climate community and beyond (National Academies of Sciences, Engineering and Medicine, 2016).

In this context, a Climate Services Toolbox (CSTools) has been developed to address this needs. The toolbox was designed to include functions for each of the main post-processing steps of seasonal forecast, but the methods are also suitable for sub-seasonal and decadal predictions. These forecasts are typically generated by running a forecast system several times using perturbations on the initial conditions and model physics (ECMWF, 2017). Each simulation is then considered a member of the ensemble. These similarities in setups among forecasts of different time horizons generally lead to common requirements in their post-processing steps (Palmer et al., 2008). Such ensembles are generated to account for initial condition and model uncertainty, to make probabilistic statements about the most likely atmospheric state (ECMWF, 2017) and to inform sensitivity studies. However, additional post-processing steps are required to translate the simulations into climate information.

CSTools is targeted primarily at applied climate scientists or climate services developers that require the use of high-quality climate data (e.g.: high-resolution data obtained by applying downscaling methods). These users can handle the tool by themselves, understanding each of the methodologies given the provided documentation and with the support of scientific research publications. The tool is fully transparent since it is open-source, allowing the user to control, understand and even adapt every step of the analysis in depth. While simple examples are given in the package documentation, this manuscript aims to showcase the usefulness of CSTools in the context of advanced state-of-the-art use cases.

1.2 From climate data to climate information

There are different forecast post-processing steps necessary to translate climate data into climate information. These steps will vary depending on the applications, but usually fall within the following categories (as illustrated on Fig. 1):

- *Data retrieval and formatting*: Optimal methods for spatial and temporal data manipulation, such as interpolation methods, are needed given the wide range of climate data formats. This can be a labour intensive step when trying to combine multiple datasets such as observations and forecasts from multiple systems.
- *Correction methods for forecast calibration*: Calibration is necessary to correct systematic errors, uncover any predictive signal and adjust forecasts to the observational statistical properties in order to be integrated into impact models. These biases originate from the approximate representation of unresolved climate processes in the forecast systems (Marcos, 2016; Van Schaeybroeck and Vannitsem, 2019; Manzanas et al., 2019).
- *Classification methods for multi-model forecast combination or scenario selection*: Combining multiple forecasting systems allows to substantially enlarge the diversity of potential weather situations (Hemri et al., 2020), errors are partially compensated and there is an increase in consistency and reliability (Hagedorn et al., 2005). Scenario selection, on the other hand, may often be useful for communication and information synthesis for specific applications (Ferranti and Corti, 2011).
- *Downscaling*: Climate forecast systems, due to computational limitations, typically provide global seasonal-to-decadal forecasts at a horizontal resolution of ~ 100 km. Users, however, require information at a finer scale. As such, statistical and stochastic downscaling techniques are commonly used to perform realistic transformations from large to small scales (Maraun and Widmann, 2018, Ramon et al. 2021).



- 85 • *Skill assessment*: Estimating the quality of the predictions is essential to understand the limitations of the simulations, to improve the current forecast systems and to provide useful forecast products tailored to several sectors (Merryfield et al., 2020). Skill estimates should be provided together with the forecast products to allow a correct interpretation of the forecasts or the added value of a system with respect to a benchmark.
- *Visualization*: From the climate services perspective, visualization tools are essential to illustrate different aspects of deterministic or probabilistic climate information.

90 Methods for each of these post-processing steps are provided within CSTools.

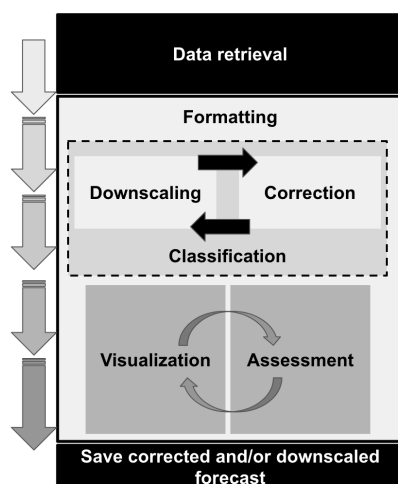


Figure 1: Scheme of the flexible CSTools workflow (from top to bottom). Each box represents a category of functions that are part of CSTools.

- 95 Several software packages are already available to analyse different types of climate data. For instance, the Earth System Model Validation Tool (ESMValTool; Eyring et al., 2016b; Eyring et al., 2020; Righi et al. 2020) was designed to facilitate the analysis of climate projections produced in the context of the Coupled Model Intercomparison Project (CMIP; Eyring et al., 2016a). The R packages s2dverification (Manubens et al., 2018), SpecsVerification (Siegert, 2017) and easyVerification (MeteoSwiss, 2017) or the python package climpred (Brady and Spring, 2021) focus on skill assessment of ensemble
- 100 forecasts. Climate4R (Iturbide et al., 2019) is an R-based framework for climate data post-processing including different methods. The main purpose of these different packages is the facilitation of research. CSTools, on the other hand, targets scientists interested in providing a climate product to some final users. CSTools could nonetheless be useful to research scientists, as it is made compatible some of the aforementioned R packages.
- 105 For a detailed description of CSTools functions and parameters, the reference manual is attached to the package and available at <https://CRAN.R-project.org/package=CSTools> in the standardized format of an R package documentation. In this manuscript, an overview of the methods and documentation gathered in CSTools is presented in Sect. 2, while the creation of a tailored dataset is shown in Sect. 3. Three case studies based on the analysis of an extreme wind speed event, the snow model SNOWPACK (Lehning et al., 2002a,b <https://models.slf.ch/p/snowpack/>) and data preparation for the hydrological model SCHEME (Baguis et al. 2010) show the usefulness of the toolbox. Section 4 concludes this paper and
- 110 discusses some future developments for the package.



2 CStools: overview

CStools was created as part of a collaborative effort between six European institutions. Given the total number of contributors and collaborators (31 in version 4.0), compiling all methods into a software package using the R statistical programming language (R Core Team, 2017) was considered the most suitable and versatile option. Creating an R package allows the inclusion of multiple tools ranging from complex statistical and climatological methods to visualization tools in the same framework. Moreover, CStools is open-source, thus allowing users and developers alike to benefit from lower costs and software flexibility, quality and reliability (Information Resources Management Association, 2013). At the same time, CStools can be integrated into other softwares in order to take advantage of its functionalities, as does, for instance, the S2S4E Decision Support Tool (<https://s2s4e-dst.bsc.es>).

CStools was developed following common guidelines agreed upon by all contributors, including conventions for adding new functionalities, and taking into account software development best practices such as the use of a Version Control System (i.e. git; Chacon and Straub, 2014), and testing with continuous integration. The use of these development guidelines has resulted in a clean and homogeneous application programming interface (API).

Most functionalities exposed to the users can be invoked and applied to complex user datasets with a single function call. For example, in order to apply a given functionality named “Func”, the user would write:

```
CST_Func(dataset, ...)
```

The “CST_*” family of functions ingest and return objects of type “s2dv_cube” (see details in Sect. 2.1), thus allowing compatibility between each functions and long post-processing chains to be created.

2.1 Technical aspects of CStools

The CStools development guidelines have been designed to maximise compatibility with other libraries such as s2dverification, s2dv and startR, all of them designed to operate fundamentally with multi-dimensional arrays with named dimensions. Because of this design, the CStools user is able to perform basic array inquiry on the “data” element of the “s2dv_cube” objects at any point in the workflow in order to check the dimensions of the data or to find the number of members, start dates or forecast lead times analysed. Internally, each of these high-level “CST_*” functions perform two nested calls to two other different but closely related functions in the package. For example, a given functionality named “Func” would involve the following function calls:

```
CST_Func(dataset, ...) {  
  ...  
  Func(dataset$data, ...) {  
    ...  
    .Func(data_array[i,], ...)  
  }  
}
```

At the most fundamental level of this nested call structure, there is a call to a basic function (e.g. “.Func”) that is designed to work with the least complex data structure possible (be it a single vector, a couple of vectors, an array and a vector, ...). At the second level is a call to a wrapper function (e.g. “Func”) around the basic function, which leverages the multiApply package (BSC-CNS et al., 2019) to extend the computation of “.Func” to inputs with any number of dimensions. The top-



level “CST_*” function is an additional wrapper function which adapts the second-level array-based function to work with “s2dv_cube” objects.

155

This nested structure has a number of benefits:

- The CSTools user code, using top-level functions, is modular, concise, readable and easy to maintain.
- The R community can easily employ it via the array-compatible low-level functions.
- Multi-core parallelism is straightforward to exploit via middle-level functions and high-level “CST_*” functions.
- In cases where the data to process is larger than the RAM memory in the workstation or the computation is very expensive, the low-level functions can be used together with the startR package (BSC-CNS and Manubens, 2020) to leverage HPC platforms and distribute workload in small chunks.

160

The modular aspect of the “CST_*” functions makes it straightforward for users to create their own post-processing workflows, as shown in Sect. 3. Metadata is propagated and expanded all along the workflows.

165

2.2 Methods in CSTools

Given that the methods included in CSTools are split into functions, the users can concatenate them to define their own post-processing workflow. This design provides flexibility allowing the users to assess the impact of the various post-processing steps by modifying the chain of functions. The users can also select a single function and apply it outside of the CSTools workflow. The functions included in the package cover fundamental loading and transformation requirements, downscaling tools, methods for correcting and evaluating forecast and advanced visualization tools (see Table 1). All functions are documented in a standard reference manual on the CRAN website (<https://CRAN.R-project.org/package=CSTools>). The documentation also includes vignettes, which are self-contained pieces of documentation combining code, text and images, describing some of the methodologies included in CSTools, as well as information on how to use the package to conduct specific analysis.

170

175

Table 1. Summary of the functions and methods by category. Prefix “CST_” refers to functions working on a specific object class called “s2dv_cube”. Asterisk indicates functions that are used in vignettes.

Retrieval and transformation	CST_Load*, CST_Anomaly*, CST_SaveExp, CST_MergeDims, CST_SplitDims, as.s2dv_cube, s2dv_cube
Classification	CST_MultiEOFS, CST_WeatherRegimes*, CST_RegimesAssign*, CST_CategoricalEnsCombination, CST_EnsClustering*
Downscaling	CST_Analogs*, CST_RainFarm*, CST_RFTemp, CST_AdamontAnalogs, CST_AnalogsPredictors
Correction	CST_BEI_Weighting*, CST_BiasCorrection, CST_Calibration, CST_QuantileMapping, CST_DynBiasCorrection
Assessment	CST_MultiMetric*, CST_MultivarRMSE*
Visualization	PlotCombinedMap*, PlotForecastPDF*, PlotMostLikelyQuantileMap*, PlotPDFsOLE, PlotTriangles4Categories*



180 2.2.1 Retrieval and transformation function

CSTools builds on the experience gained from the development of other R packages for climate data analysis, such as s2dverification. Specifically, CSTools has adopted its “s2dv_cube” object as a central data structure to represent and carry data and metadata across function calls. A “s2dv_cube” object is essentially a R list which includes a multi-dimensional array of climate data originating from either observations or forecasts, and metadata, such as time period or region covered,
185 dataset and variable name, and units. The development guidelines define conventions to ensure “s2dv_cube” objects are used in a coherent way throughout the package.

CSTools has a single but powerful function to retrieve data from netCDF files called *CST_Load*. This function is a wrapper of the s2dverification *Load* function which allows reading monthly or daily data from a set of specified forecast datasets
190 together with specified date-corresponding observations (Manubens et al., 2018). This function makes use of the Climate Data Operators software (CDO; Schulzweida, 2019) to automatically interpolates all the data onto a common grid. Three samples of “s2dv_cube” objects created from using *CST_Load* are provided along with the package: *area_average*, with forecast and observational climate data averaged over a region; *lonlat_data* and *lonlat_prec* containing forecast and observational climate data for temperature and precipitation.

195 Although datasets can be retrieved from OPeNDAP URLs with NetCDF files, in general, the datasets have to be downloaded onto a local repository and formatted to comply with the *CST_Load* requirements. Observational reference datasets are stored in a folder in separate monthly NetCDF files (other formats are also possible; see https://earth.bsc.es/gitlab/es/s2dverification/-/blob/master/vignettes/data_retrieval.md for more information), while seasonal
200 forecasts are stored by start date in distinct folders (see https://cran.r-project.org/web/packages/CSTools/vignettes/Data_Considerations.html). A python code to download and format the seasonal forecast datasets from the CDS is provided in the repository CDS Seasonal Downloader (<https://earth.bsc.es/gitlab/es/cds-seasonal-downloader>).

205 For users who retrieve data by other means (e.g. using the library *ncdf4*; Pierce, 2019), the CSTools package contains two functions to convert data to a “s2dv_cube” object. If the data and metadata have been loaded in separate objects, they can be merged into a “s2dv_cube” object with the function *s2dv_cube*. On the other hand, if the data and metadata have been loaded into a single object, it can be transformed into class “s2dv_cube” class with the *as.s2dv_cube* function.

210 One of the capabilities of CSTools is to create a new dataset after, for example, the data has been downscaled and/or calibrated. In that case, the user may need to save the new dataset into files to be shared among other users or its community. Therefore, the package comes with a saving function called *CST_SaveExp* which creates netCDF files in a directory set by the user and which can be loaded again with the *CST_Load* function. Moreover, the climatological essential steps of computing anomalies can be done with *CST_Anomaly* which is a wrapper function of s2dverification methods that also
215 allows computing smoothed climatologies.

The functions *CST_MergeDims* and *CST_SplitDims* provide additional flexibility to manipulate “s2dv_cube” objects. For instance, it is commonly required to split the time dimension of annual data into two dimensions, one identifying the season and the other the month of that season. On the contrary, some advanced classification methods may need to merge the
220 latitudinal and longitudinal coordinates in a single dimension.



2.2.2 Classification methods

Classification methods are widely used in climatology to summarize the climatological conditions captured by observations or simulations. Sokal (1966) was already using sophisticated univariate and multivariate climatic classification systems to be generated from enormous data bases (Balling, 1984). However, the functions included in CSTools for this purpose are modern methods adapted to observations, reanalyses and climate model outputs with multiple ensemble members.

The *CST_MultiEOFs* function allows conducting Empirical Orthogonal Functions (EOF) analysis simultaneously over multiple variables. Based on singular value decomposition, the EOF analysis is applied over the region of interest (for example the Mediterranean region) in order to define, for each of the N variables chosen, a reduced phase space based on the leading modes of variability. A simultaneous analysis of these fields is then carried out with a (multivariate) EOF analysis in the subspace spanned by the leading EOFs of each field. This produces a N-variable EOF picture of the variability in the region. The associated principal components can represent multi-variable indices that can be used to verify the forecast.

CST_WeatherRegimes and *CST_RegimesAssign* are complementary functions to derive weather regimes (Cortesi et al., 2019; Torralba, 2021). The first function computes a set of weather regimes using a cluster analysis. The dimensionality of this object can also be reduced by using PCs obtained from the application of the EOF analysis to filter the dataset, while the cluster analysis can be performed with the traditional k-means or hierarchical clustering. On the other hand, *CST_RegimesAssign* matches anomalies to a set of reference maps obtained using *CST_WeatherRegimes*. The anomalies are assigned to the most similar reference map using either the minimum Euclidean distance or the highest spatial correlation, which can be particularly useful to classify the predictions according to the clusters identified in the observational reference.

CST_CategoricalEnsCombination converts a multi-model ensemble forecast into a categorical forecast by giving the probability for each category. Different methods are available to combine the different ensemble forecasting models into probabilistic categorical forecasts. The amount of categories can be changed and are taken as the climatological quantiles (e.g. terciles), extracted from the observational data. The available methods are: “pool” for ensemble pooling where all ensemble members of all forecast systems are weighted equally; “comb” for a model combination where each model system is weighted equally; and “mmw” for model weighting. The model weighting method is described in Rajagopalan et al. (2002), Robertson et al. (2004) and Van Schaeybroeck and Vannitsem (2019). More specifically, this method uses different weights for the occurrence probability predicted by the available models and by a climatological model and optimizes the weights by minimizing the ignorance score.

CST_EnsClustering is a cluster analysis tool, based on the k-means algorithm, for ensemble predictions. The aim is to group ensemble members according to similar characteristics and to select the most representative member for each cluster. The user chooses which feature of the data is used to group the ensemble members by clustering (e.g. temporal mean). The anomaly is computed with respect to the ensemble members and the EOF analysis is applied to these anomaly maps. After reducing dimensionality via EOF analysis, k-means analysis is applied using the desired subset of PCs. The user can choose how many Principal Components (PCs) to retain or the percentage of explained variance to keep for the EOF analysis.

2.2.3 Downscaling methods

Downscaling is designed to increase the resolution of a dataset. In a climate service chain, downscaling is a fundamental step to transform the climate simulations from their coarse resolution to the finer resolution required by many final users studying regional environmental changes (Maraun et al. 2010; Rössler et al., 2019). CSTools contains five different downscaling methodologies based on analog techniques, stochastic simulations or regression.



265 The *CST_Analogs* function can be used to downscale any gridded dataset using analogs. The function, based on the method of Yiou et al. (2013), searches for days with similar large-scale conditions to provide high-resolution fields over a specific region. Regions and variables can be defined by the user and three different criteria to select the analogs are available: (1) minimum Euclidean distance in the large-scale pattern, (2) minimum Euclidean distance in a large-scale pattern and in a local-scale pattern, and (3) minimum Euclidean distance in a large-scale pattern and a local scale pattern as well as maximum correlation in a local variable to be downscaled.

270

CST_RainFARM implements a stochastic downscaling technique and represents a so-called full-field weather generator. More specifically, this function generates synthetic fine-scale precipitation fields whose statistical properties are consistent with the small-scale statistics of observed precipitation, while preserving the properties of the large-scale precipitation field. The Rainfall Filtered Autoregressive Model (RainFARM; Reborá et al. 2006a,b) is based on the nonlinear transformation of a linearly correlated stochastic field generated by small-scale extrapolation of the Fourier spectrum of a large-scale precipitation field. Developed originally for downscaling data at weather timescales, the method has been adapted for downscaling at climate timescales by D'Onofrio et al. (2014) and recently improved for regions with complex orography (Terzago et al., 2018). This methodology relies on two distinct functions to compute weights from high-resolution climatologies (*CST_RFWeights*) and the spatial-spectral slope used to extrapolate the Fourier spectrum to the unresolved scales (*CST_RFSlope*).

280

CST_RFTemp implements a simple lapse rate correction to a near-surface temperature field to account for changes in orography between a low and high resolution gridded dataset.

285 ADAMONT (ADApTation of RCM outputs to MOuNTain regions; Verfaillie et al., 2017) is a downscaling method designed to adjust forecasts of daily variables. The method is based on the quantile mapping approach and originally relied on a regional reanalysis of hourly meteorological conditions. Two functions to implement ADAMONT have been included in CSTools. *CST_AdamontQQcor* computes a quantile mapping based on weather types for forecast data while *CST_AdamontAnalog* uses these weather types to find analogous data in the reference dataset.

290

The *CST_AnalogsPredictors* function downscales precipitation or maximum/minimum temperature low resolution forecast output data, in a domain centred over Iberian Peninsula, through the association with an observational high resolution dataset (Peral García et al., 2017) and a collection of predictors and reference synoptic situations similar to the estimated day. As a first step, a partner function *AnalogsPredictors_train* must be run to compare the large-scale atmospheric circulation to each of the atmospheric configurations from a reference period. The most similar days, defined by the Euclidean distance of winds, are chosen as their analogs.

295

2.2.4 Correction methods

Correction methods can improve the quality of simulations by reducing the systematic errors that are present in the forecast due to model deficiencies. The periodicity of modes of variability (i.e. space-time patterns that tend to recur in the observed record) can also be exploited to improve the forecast skill.

300

Best Estimate Index (BEI) is a methodology that can be used to improve the forecast skill when a relationship exists between a climatological index and a given climate variable as shown in Sánchez-García et al. (2019), where the technique is shown to improve the skill for precipitation over the Iberian Peninsula using the North Atlantic Oscillation (NAO). The



305 methodology consists of three functions: *BEI_PDFBest* combines the NAO signals from the two forecast systems, *BEI_Weights* provides the weights to correct a forecast system and *CST_BEI_Weighting* computes the ensemble mean or the tercile probabilities considering the weights returned by *BEI_Weights*.

Calibration can be considered as a way of obtaining predictions with average statistical properties similar to those of a
310 reference data set. *CST_Calibration* performs the correction on the forecast systems' simulations using five different member-by-member methodologies: the "bias" method corrects the mean bias only, the "evmos" method applies a variance inflation technique to ensure the correction of the mean and the correspondence of variance between forecasts and observations (Van Schaeybroeck and Vannitsem, 2011). The ensemble calibration methods "mse_min" and "crps_min" correct the bias, the overall forecast variance and the ensemble spread as described in Doblas-Reyes et al. (2005) and Van
315 Schaeybroeck and Vannitsem (2015), respectively. While the "mse_min" method minimizes a constrained mean-squared error using three parameters, the "crps_min" method features four parameters and minimizes the Continuous Ranked Probability Score (CRPS). The "rpc-based" method adjusts the forecast variance to ensure that the ratio of predictable components (RPC) is equal to one (Eade et al., 2014). The function allows the five calibration methods to be performed in leave-one-out cross-validation mode, which means that the observed value of the year that is being corrected is not
320 considered in the calibration, as it would be the case for real-time forecasts (Doblas-Reyes et al., 2005, Torralba et al., 2017). The use of cross-validation is particularly important in order to avoid overestimating the skill when the hindcasts are calibrated. *CST_BiasCorrection* performs the same analysis as *CST_Calibration* using the "evmos" method but allowing to calibrate either a hindcast or forecast.

325 *CST_QuantileMapping* performs a quantile mapping adjustment by matching the probability distribution of a forecast with the probability distribution of a set of observations. The function in CSTools calculates the relation between a set of past forecasts (i.e. hindcasts) and observations and applies the correction to the hindcast itself or to a different forecast. This function relies on the R package qmap (Gudmundsson et al., 2012; Gudmundsson, 2016). The user can set several parameters to define the distance between quantiles when adjusting the distribution, or the sample length in cases when the
330 user wants to split the temporal dimension to apply separate adjustments.

CST_DynBiasCorrection relies on the dynamical state of the system to correct the systematic errors rather than on its statistical properties. This method uses two dynamical system metrics to correct the bias of each ensemble member: the local (in phase space) dimension and the persistence. In simple terms, they describe the recurrences of a system around a state in
335 phase space. Dimension provides information on how the system can reach a state and how it can evolve from it. Thus, dimension is a proxy for the system's active number of degrees of freedom. A very persistent state is typically highly predictable, while a very unstable state yields low persistence (Faranda et al., 2017; Faranda et al., 2019). The functions *CST_ProxiesAttractor* (to compute local dimension d and inverse of persistence θ) and *Predictability* (to compute scores of predictability based on the dynamical indicators resulting from *CST_ProxiesAttractor*) are internally used by
340 *CST_DynBiasCorrection* and they are also exposed for users interested in interpreting the method's intermediate results.

2.2.5 Verification functions

Verification is not the main objective of this package. For that purpose, we refer users to other R packages such as s2dverification, SpecsVerification and easyVerification. However, in order to facilitate the evaluation of the forecasts, some
345 basic metrics have been included.



CST_MultiMetric calculates correlation, root mean square error and the root mean square error skill score for individual models and multi-model mean (if desired) with the observations (Mishra et al., 2019) and the ranked probability skill score (RPSS) based on terciles.

350

CST_MultivarRMSE calculates the RMSE using multiple variables, as the mean of each variable's RMSE scaled by its observed standard deviation. Variables can also be weighted based on their relative importance (as defined by the user).

2.2.6 Visualization

355 Some of the most requested functionalities in climate services are data visualization tools that allow presenting large quantities of information in an intuitive way. All the visualization functions in CStools can be customized by modifying colours, titles, sizes, etc. and it is possible to save them to files in different formats (e.g. .ps, .eps, .png, pdf, ...) or display the result in a pop-up window.

360 *PlotCombinedMap* combines multiple 2-dimensional datasets into a single map based on a decision function. In other words, several "maps" are provided as input, and for each "map" the function creates a colour legend. A decision function is used at each gridpoint to choose the value to be displayed, in the process retaining the information of which "map" it belongs to. For instance, multiple model skills could be compared in a region to visualize which is the best model in each region (Mishra et al., 2019; Torralba et al., 2021). Other applications, such as comparing multiple variables, are also possible.

365 *PlotMostLikelyQuantileMap* allows visualizing different probabilities easily. It receives as main input (via the parameter "probs") a collection of longitude-latitude maps, each containing the probabilities (from 0 to 1) of the different grid cells belonging to a category: terciles, quantiles, or others (Lledó et al., 2020a; Torralba, 2019). The function plots the probability for the category with the maximum probability in each grid point.

370 *PlotForecastPDF* plots the probability distribution function of several ensemble forecasts in separate panels. By default, the function plots the ensemble members, the estimated density distributions and the tercile probabilities. Probabilities for extreme categories, above (below) the 90th (10th) percentile (from now on, P90 (P10)), and observed values can also be included. This function is useful to compare changes in forecasts with different lead times (Soret et al., 2019). A comparison between forecasts from different models, different modes of variability (Lledó et al., 2020a) or even forecasts at different
375 locations are also possible.

PlotPDFsOLE plots two probability density Gaussian functions and their combination by the optimal linear estimation (OLE). The mean and the standard deviation of the two probability functions must be provided (Sánchez-García et al., 2019).

380

It can sometimes be useful to present tabular results as colours instead of numbers. For this purpose, *PlotTriangles4Categories* converts a 3-dimensional numerical data array into a coloured grid with triangles. This function can be used to quickly compare modes of variability, skill metrics, differences between methods or forecast systems as a function of the lead times or seasons (Torralba, 2019; Verfaillie et al., 2021; Lledó et al., 2020b).

385

Examples of these visualisation tools as well as other functions of the package are shown through the two example case studies provided in the next section.



3 Use Cases

In order to demonstrate how CSTools can be used to provide climate information to potential users, we present three case studies which rely on CSTools for data post-processing. The first case study assesses whether seasonal forecasts could anticipate the very strong near-surface winds over the Iberian Peninsula in March 2018 such as to provide useful information to the energy sector. In the second case, precipitation seasonal forecasts are post-processed following the requirements to use them to drive model of snowpack depth in high mountain sites. Finally, we provide an example of how seasonal forecasts of rainfall and near-surface temperature can be post-processed to drive a hydrological model.

3.1 Use case 1: Assessing the odds of an extreme event

This case study showcases the steps required to analyse a high-impact event using seasonal forecasts initialized one to three months in advance. In March 2018, the Spanish Meteorological Agency activated its protocol of early warning system for 47 regions of Spain due to the high-speed winds forecasted and possible coastal impact (<https://www.elperiodico.com/es/tiempo/20180311/felix-pone-en-riesgo-a-47-provincias-por-vientos-que-podran-alcanzar-los-140-km-h-668171>). Very high wind speeds were later recorded over large part of the Iberian Peninsula due to 4 cyclones going across the IP (AEMET, 2018).

This type of event is of interest to the energy sector, given its impacts on wind power generation, energy demand and electricity prices, and such interest is likely to keep rising as we continue transitioning towards, and become more reliant on, renewable energy. For context, the renewable energy production had grown substantially in Spain over the course of 2017-18: renewable energy generation was 51.1 % higher in March of 2018 compared to what it had been during the same month of the previous year. A historical maximum of monthly renewable generation was hit with 13,204 GWh (33.1 % of share), of which wind energy contributed 7,676 GWh, setting also a new record of monthly wind generation (Red Eléctrica España, 2018). These high amounts of renewable generation in March 2018 resulted in an important drop in electricity prices. Because of its strong impact on the market, there is a lot of interest in the energy sector to anticipate this type of events.

The use case presented here shows whether the 2018 event had been anticipated by ECMWF System 5 a few months in advance. We note that the code could be adapted to other regions, time periods and variables and a detailed description of the code is provided below for users interested in modifying the necessary parameters. First, the seasonal forecasts initialized in December 2017, January 2018 and February 2018 are bias adjusted and assessed. Two functions from CSTools are used to post-process the wind speed seasonal forecasts: *CST_Load* and *CST_BiasCorrection*. The key decisions are the parameters used to retrieve the data from files to achieve a coherent analysis of the March 2018 event (Fig. 2). The analysis is repeated for three different start dates (i.e. December, January and February). For each start date, three different data types are loaded: the hindcast, i.e. retrospective forecasts initialized in the past for start dates ranging from 1993 to 2016 for December initialization and 2017 for January and February initializations; the observational reference, covering the same period as the hindcast; and the operational forecast, i.e. the latest simulations initialized just before the event (i.e. December 2017, January 2018 and February 2018). In all the data loading calls, the same region must be requested through the parameters *lonmin*, *lonmax*, *latmin* and *latmax* of the function *CST_Load*, in which the output type required is gridded data rather than area average by setting *output* parameter as “lonlat”.

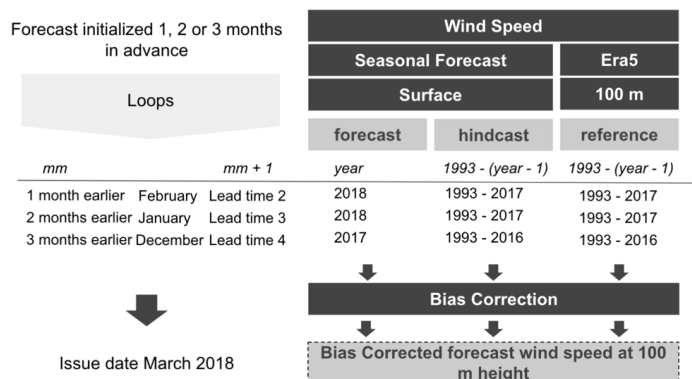


Figure 2: Scheme of the methodology applied. Grey boxes indicate the data, methods and results. The required parameters to analyse the March 2018 event are specified for the simulations initialized one, two and three month(s) in advance on white background.

430

For both the hindcasts and the forecasts, we use monthly means of 10 m wind speed from the ECMWF SEAS5 system, obtained from C3S (SEAS5) at 1° spatial resolution. For the observational reference, we use monthly mean 100 m wind speeds from the ERA5 reanalysis (Hersbach et al., 2020) at 0.25° (around 30 km) spatial resolution. Winds at 100 m height are of relevance for energy applications and, although this variable is not available directly from the seasonal prediction system, the bias adjustment procedure will convert 10 m to 100 m winds by assuming a logarithmic wind profile (Drechsel et al., 2012). The different variable names must be specified in the *CST_Load* call through the parameter *var*, since the function needs to read the correct variable written on the NetCDF files in the data storage. Therefore, the *var* parameter is set to “sfcWind” when retrieving hindcasts and forecasts, while for the reference dataset it is set to “windagl100”. Given the difference in spatial resolution, a regridding of the reference dataset is also requested by the parameter *grid*. The path pointing to the simulations and the reference are also passed to the *CST_Load* function through parameters *exp* and *obs*, respectively. Notice that the labels \$STORE_FREQ\$, \$VAR_NAMES\$, \$START_DATES\$, \$YEARS\$ and \$MONTHS\$ are used when defining the paths. These labels will be interpreted and substituted by the function following the information provided by the other parameters of *CST_Load*.

435

440

445

An index *mm* indicating the number of preceding months (*mm*) is introduced to loop over the three start dates in order to simplify the code. When *mm* is 1, the bias adjustment for March with the forecasts initialized one month in advance (i.e. the February start date) is computed. The target year is set in the “year” variable as 2018. The start dates of the simulations to be loaded are created and stored in the “hcast_sdates” and “fcst_sdates” variables, which correspond to a vector of dates for the 1st of February from 1993 to 2017 and the 1st of February 2018, respectively. For the February start date, the lead time two (i.e. *mm* + 1) corresponds to the forecast for March which is selected through the *leadtimemin* and *leadtimemax* parameters.

450

Finally, a simple bias-correction method (*CST_BiasCorrection*) is used to compute the biases between the hindcast and the reference datasets and then apply a correction to the mean and standard deviation of the forecast dataset by. The results of each loop are stored in a list.

455

460

```
library(CSTools)
exp_path <- list(name = "ECMWF5",
  path =
"/esarchive/exp/ecmwf/system5c3s/$STORE_FREQ$_mean/$VAR_NAME$_f6h/$VAR_NAME$_$START_DATES.nc")
obs_path <- list(name = "ERA5",
  path =
"/esarchive/recon/ecmwf/era5/$STORE_FREQ$_mean/$VAR_NAME$_f1h/$VAR_NAME$_$YEAR$MONTH$.nc")
# Target months March (3)
# Assess forecast from 1 to 3 months in advance
```



```
465 months_in_advance <- c("02", "01", "12")
    for (mm in 1:3) {
      # Generate the start dates of hindcast period
      year <- ifelse(mm == 3, 2017, 2018)
      hcst_sdates <- paste0(1993:(year - 1), months_in_advance[mm], "01")
470 # Load hindcast data
      wind_hcst <- CST_Load(var = "sfcWind", exp = list(exp_path),
                           sdates = hcst_sdates, nmember = 25,
                           leadtimemin = mm + 1, leadtimemax = mm + 1,
                           storefreq = "monthly", sampleperiod = 1,
475 latmin = 36, latmax = 44, lonmin = -10, lonmax = 4,
                           output = "lonlat")

      # Generate the start dates of forecast period
      fcst_sdates <- paste0(year, months_in_advance[mm], "01")
      # Load forecast data
480 wind_fcst <- CST_Load(var = "sfcWind", exp = list(exp_path),
                          sdates = fcst_sdates, nmember = 25,
                          leadtimemin = mm + 1, leadtimemax = mm + 1,
                          storefreq = "monthly", sampleperiod = 1,
485 latmin = 36, latmax = 44, lonmin = -10, lonmax = 4,
                          output = "lonlat")

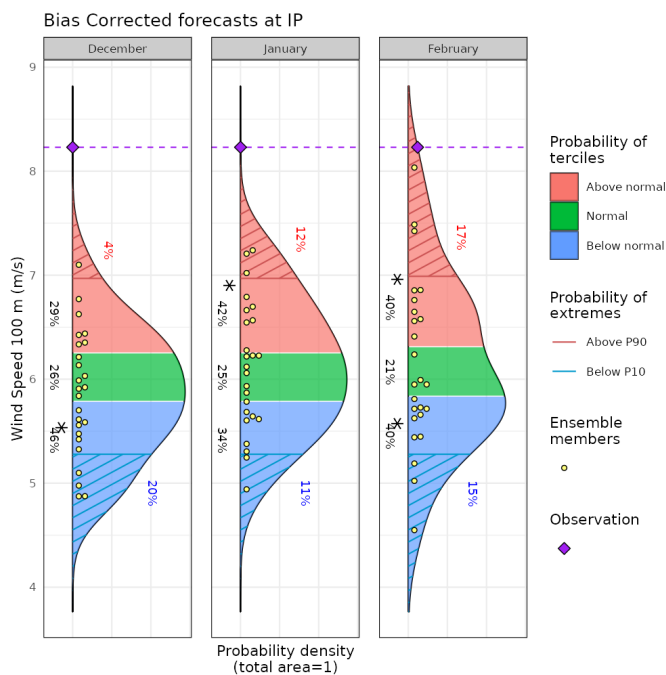
      # Load reference data
      wind_ref <- CST_Load(var = "windagl100", obs = list(obs_path),
                           sdates = hcst_sdates, nmember = 1,
                           leadtimemin = mm + 1, leadtimemax = mm + 1,
490 storefreq = "monthly", sampleperiod = 1,
                           latmin = 36, latmax = 44, lonmin = -10, lonmax = 4,
                           output = "lonlat",
                           grid = "r360x181")

      # Bias Adjustment
495 wind_fcst <- CST_BiasCorrection(exp = wind_hcst,
                                   obs = wind_ref,
                                   exp_cor = wind_fcst)

      wind_fcst_BC[[mm]] <- wind_fcst
    }
500
```

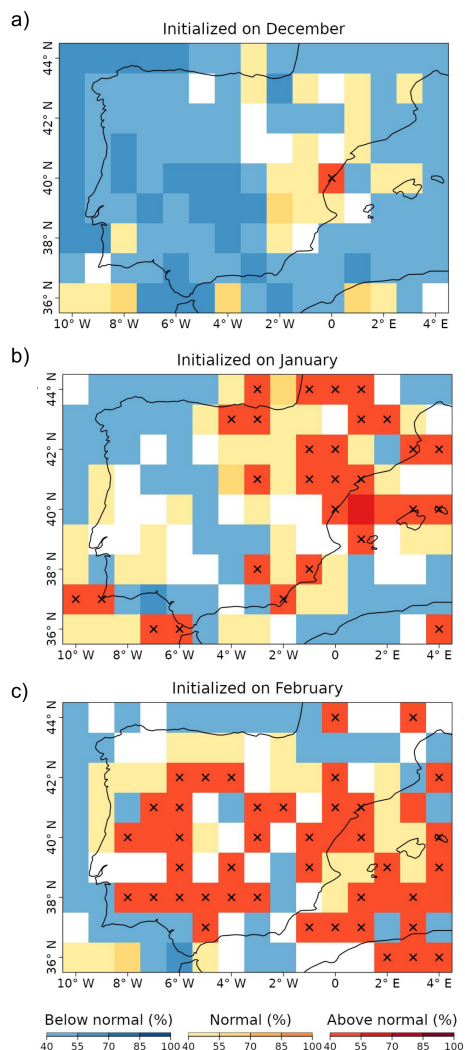
Once the forecasts are post-processed, additional CSTools functions can be used to visualize the forecast distributions. The *PlotForecastPDF* function, for instance, compares the probability distribution function of the March 2018 100 m wind speed forecasts issued 1 to 3 month(s) in advance (Fig. 3). Three months in advance, only one member exceeds the P90. The simulations initialized one and two month(s) in advance suggest a weak shift towards above-normal conditions (~40 % probability of the above normal tercile) and towards extreme high values (12 % and 17 % exceeding P90). Moreover, the forecast's tercile probabilities do not indicate a shift towards above-normal winds as lead time decreases (the January start date suggests a slightly larger probability of above-normal winds than the February start date). Even though for start dates in both January and February three members exceed P90, the corresponding probabilities are different due to the ensemble dressing applied. In February, the probability of observing extreme wind conditions was almost twice as large as in January.

510 Individual ensemble members typically also suggest much weaker wind speed anomalies than observed, except for one member in the February initialization, indicating that in this case the prediction system anticipated this situation as a potential outcome.



515 **Figure 3: Seasonal forecasts of wind speed at 100 m height, averaged over 10 °W-4 °E and 36-44 °N for March 2018. Each panel corresponds to forecasts launched 3 to 1 month(s) ahead (from left to right). Methodology: simple bias correction with ERA5 observations, based on previous hindcasts since 1993. An asterisk indicates the tercile with the highest probabilities.**

520 The spatial distribution of the tercile probabilities can be displayed with the *PlotMostLikelyQuantileMap* function (Fig. 4). An extra layer has been included to mark with crosses the grid points where observations agree on the most likely tercile indicated by the forecast. Three months in advance, most of the region shows that the tercile of highest probability is the below-normal category. One and two month(s) in advance, the colours shift towards the normal and above-normal categories. In the January simulation, the eastern region presents more above-normal probability of high wind speed values than the western region. In the February simulation, the above-normal probability class is widespread on the whole Iberian Peninsula.



525

Figure 4: Probabilities of the most likely tercile for the March 2018 100 m wind speeds, as indicated by the forecasts issued 3 to 1 month(s) ahead (top to bottom). The crosses indicate that the observations fell into the most likely tercile displayed by the forecast. White grid points indicate that no tercile category has more than 40 % of probability.

530 Users that can benefit from climate information, such as stakeholders (e.g. energy system planners), are usually not familiar
with probabilistic forecasts and the added value that it could potentially bring to their planning. In order to become more
autonomous in their decision making, a learning process could be started based on relevant show-case climate events such as
the one provided here. Therefore, such use case could be of interest for climate services developers that need to post-process
a seasonal forecast variable and present the results in a concise yet user-friendly manner with a reduced number of images
535 and tables.

When an unsatisfactory outcome happens because of unfavourable atmospheric conditions, even including a seasonal
forecast in the decision strategy, this code could be used to evaluate whether the seasonal forecast included the possibility of
an unsatisfactory outcome, whether other variables were better capturing the situation in that case, or if a different bias



540 correction method would improve the skill of the seasonal forecast. Furthermore, it is possible to easily modify this code to
 compare the results provided by different models.

3.2 Use case 2: Seasonal forecast of snow depth and snow water equivalent in high-elevation sites

Snowpack in the mountains represents an essential water reservoir that is fed by snowfall during the cold season and then
 released in late spring and summer. Mountain meltwater is essential for several economic activities including hydropower
 generation, agriculture, industry, and meltwater shortage can induce strong economic losses. Therefore, reliable seasonal
 545 forecasts of snow resources that, at the beginning of the snow season (November) estimate the snow accumulation towards
 the end of spring (April-May), are highly pursued. These would allow water management authorities and hydropower
 companies to implement early water management plans several months ahead of a water-demand peak and mitigate the
 effects of a possible water shortage. To support this need, a modelling chain driven by seasonal forecasts of meteorological
 550 variables from the C3S seasonal forecasting systems was developed, employing the physical 1-dimensional snow model
 SNOWPACK (Bartelt and Lehning, 2002), to estimate snow depth and snow water equivalent at selected high-elevation
 sites in the North-Western Italian Alps. A general scheme of this application is shown in Fig. 5. Important decisions include
 the downscaling method, the target region, the simulation and observation datasets as well as the season of interest. In this
 case, the region is the Alpine mountain range in central Europe (42-49 °N, 4-11 °E), including the high-elevation stations for
 555 which the SNOWPACK model is run.

The RainFARM downscaling method incorporated within CStools is employed to downscale precipitation which is then
 used as input for the SNOWPACK model. This method allows taking into account the orographic effects on the precipitation
 distribution and generates a user-defined number of stochastic downscaling realizations for each member of the original
 560 seasonal forecast simulations. For each ensemble member of the seasonal forecast model, we generate 10 stochastic
 downscaling realizations. In the following subsection, we present the method applied to the SEAS5 model providing 25
 ensemble members, such that at the end of the downscaling procedure we obtain a total of 250 fine-scale precipitation fields.

Since the RainFARM downscaling relies on the estimation of the spatial power spectrum of precipitation fields, a squared
 565 domain is required. Moreover, this domain has to be larger than the target study area to avoid artifacts/border effects within
 the target area. The target season is winter, so the 1st November start date simulations available for the period 1993-2018 are
 considered. Daily precipitation data of SEAS5 are downscaled from the original 1° spatial resolution. The reference datasets
 employed are i) ERA5 daily precipitation reanalysis at 0.25° (around 30 km) spatial resolution (Hersbach et al., 2020) for the
 bias correction and for the estimation of the spectral slopes and ii) the WorldClim2 monthly climatology at 1 km spatial
 570 resolution (Fick and Hijmans, 2017) for generating the precipitation weights to obtain a more realistic distribution.

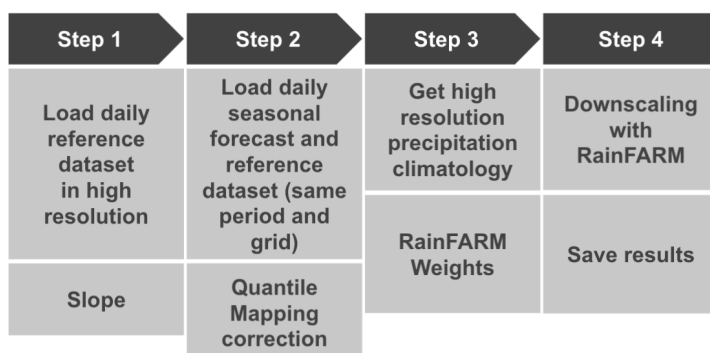




Figure 5: Scheme of the steps that need to be carried out to obtain and save a downscaled precipitation dataset. These steps are explained in detail in the text of the manuscript.

575 In the scheme (Fig. 5), three steps should be carried out before applying the RainFARM method. In steps 1 and 3, necessary parameters are computed: the spectral slopes and the orographic weights; quantile mapping correction is applied to the seasonal forecast in order to correct the bias of the model in step 2, and the downscaling is computed in step 4.

580 All computations performed in the first step only require the CSTools package. As mentioned above, the spectral slope is calculated using ERA5 at its original resolution and over a larger domain than the target region (37.5-53.25 °N, 2.5-18.25 °E). The path pattern to the data is defined using labels: \$STORE_FREQ\$, \$VAR_NAME\$, \$YEAR\$ and \$MONTH\$. These labels will be interpreted by *CST_Load*. For instance, the \$VAR_NAME\$ will be substituted by the information passed by the parameter *var* which in this case is “prlr” that stands for precipitation rate and the \$YEAR\$ and \$MONTH\$ will be interpreted from the *CST_Load sdates* parameter which requires a vector of dates in the format “YYYYMM01”
585 where YYYY is the year and MM the month. Then, *CST_Load* retrieves the data from files and arranges it with the following dimensions: *dataset* of length 1 since only ERA5 is being requested, *member* = 1 since this reanalysis only provides one simulation, *sdate* dimension is of length 312 which corresponds to the 26 years of 12 months defined in object “years” with an *ftime* dimension up to 31 corresponding to each day of the month. The remaining dimensions, *lat* and *lon* correspond to the squared domain requested in *CST_Load*. Given that *CST_Load* splits the time series among *sdates* and
590 *ftime* dimension when specifying a forecast dataset, our ERA5 path pattern has been requested through this option. On the other hand, specifying the ERA5 path pattern as an observational dataset (in the *obs* parameter), the function will return a continuous time series from 1993 to 2018 which is less convenient for our purposes here.

In this example over the Alpine domain, the slope of the spatial power spectrum of ERA5 daily precipitation at 0.25°
595 exhibits temporal variability at the seasonal scale. In order to account for this, we calculate the spectral slopes at the monthly time scale, fitting wavenumbers 5 and higher (scales smaller than about 250 km) in order to better reproduce the slope of the spectrum at the small scales (see Terzagó et al., 2020 for details). The result of this code are the spectral slopes from January to December.

```
600 library(CSTools)
era5 <- list(name = "era5", path = "/esarchive/recon/ecmwf/era5/$STORE_FREQ$_mean/$VAR_NAME$_f1h-
r1440x721cds/$VAR_NAME$_YEAR$MONTH$.nc")
years <- unlist(lapply(1993:2018, function(x){paste0(x, sprintf("%02d", 1:12), "01"))})
605 era5 <- CST_Load(var = "prlr", exp = list(era5), sdates = years, nmember = 1,
storefreq = "daily", sampleperiod = 1,
latmin = 37.5, latmax = 53.25, lonmin = 2.5, lonmax = 18.25,
output = "lonlat")
era5 <- CST_SplitDim(era5 split_dim = "sdate", indices = rep(1:12, 26))
slope <- CST_RFslope(era5, time_dim = c("sdate", "ftime"), kmin = 5)
```

610 **Code Step 1.**

In the second step, we load the data, taking advantage of library *zealot* (Teetor, 2018) that allows us to simplify our code by using an advanced version of the assignment operator (%<-%). Again, the paths to the necessary data must be defined using labels: for the forecast data the path points to the SEAS5 dataset while for the reference data the path points to the ERA5
615 reanalysis. Thanks to *CST_Load*, these datasets could be reshaped onto a common grid, which, by default, is the grid of the first dataset provided, i.e. the SEAS5 grid. The vector “StartDates” which defines the period of study for November 1st simulations, is then assigned to the *sdates* parameter.



620 In order to apply the quantile-mapping correction month by month, the function *CST_SplitDim* is used to divide the forecast
time dimension in two: one for identifying the days of the month and another to store each month separately. The result of
step 2 is a bias-corrected forecast consistent with the reference dataset: the forecast probability density function matches the
one for the references, resulting in the same climatology. A simple visual evaluation of the impact of the quantile mapping
correction is shown in Fig. 6.

625

630

635

640

```
library(zeallot)
StartDates <- paste0(1993:2018, "1101")
exp <- list(name = "ecmwfS5", path =
"/esarchive/exp/ecmwf/system5c3s/$STORE_FREQ$_mean/$VAR_NAME$_s0-24h/$VAR_NAME$_$START_DATE$.nc")
obs <- list(name = "era5", path =
"/esarchive/recon/ecmwf/era5/$STORE_FREQ$_mean/$VAR_NAME$_f1h-r1440x721cds/$VAR_NAME$_$YEAR$$MONTH$.nc")
c(exp, obs) %<- CST_Load(var = "prf", exp = list(exp), obs = list(obs),
sdates = StartDates, nmember = 25,
storefreq = "daily", sampleperiod = 1,
latmin = 42, latmax = 49, lonmin = 4, lonmax = 11,
output = "lonlat", nprocs = 1)
exp <- CST_SplitDim(exp, split_dim = "ftime")
obs <- CST_SplitDim(obs, split_dim = "ftime")
exp.qm_months <- CST_QuantileMapping(exp, obs, method = "QUANT", wet.day = FALSE,
sample_dims = c("member", "sdate", "ftime"))
exp.qm <- CST_MergeDims(exp.qm_months, merge_dims = c("ftime", "monthly"),
na.rm = TRUE, ncores = 4)
```

Code Step 2.

645 Step 3 computes the orographic weights from a fine-scale precipitation climatology. In this case, the WorldClim2 dataset
precipitation at 30 seconds resolution is used although other climatologies at high resolution could be used. The WorldClim2
dataset is formatted in tiff files that can be automatically downloaded in the R session thanks to the raster library (Hijmans,
2020). The piece of code for Step 3 shows how to compute the orographic weights for all individual months at once: getting
the data from the remote dataset, subsetting for the Alps region with a small increment to correctly compute interpolation
650 (3.5-11.5 °E, 41.5-49.5 °N), and storing the data in an “s2dv_cube” object to be passed to *CST_RFWeights*.

The target resolution is the one most suitable for each specific application. To run the SNOWPACK model, we are interested
in the local scale and we choose a target resolution of 0.01°, corresponding to about 1 km. Therefore, the weights and the
RainFARM method (step 4) would be computed with a refinement factor (*nf*) 100. However, such a high refinement factor
655 implies a rather large computational load, and here we show the code using a refinement factor 4. We recommend the users
to approximately calculate the expected size of the final output, as follows: the original data input to the downscaling step
has 25 members, 26 start dates, 31 daily lead times on 8 months covering a region of 8 by 8 grid points, which 8 times its
product is ~ 80 MB; this size will increase by a factor 10 since the realizations and the refinement factor will be applied on
both spatial dimensions. For a refinement factor of 100 (4), the expected output is ~80 MB x 10 x 100 x 100 (~ 80 MB x 10
660 x 4 x 4), so around 8 TB (12.5 GB). The users need to consider that the data size also has implications on the computation
time. The result of step 3 is an array with spatial dimensions and an extra dimension for each month containing the weights
for which values greater (lower) than 1 will amplify (reduce) the precipitation signal from the seasonal forecast (Fig. 6).

665

670

```
# WorldClim data to s2dv_cube
library(raster)
worldclim <- getData("worldclim", var = "prec", res = 0.5, lon = 5, lat = 45)
wc_month <- lapply(1:12, FUN = function(x) {
res <- crop(worldclim[[x]],
extent(3.5, 11.5, 41.5, 49.5))
res <- as.array(res)
names(dim(res)) <- c("lat", "lon", "month")
return(res)
})
```



675

```
xy <- xyFromCell(crop(worldclim[[1]], extent(3.5, 11.5, 41.5, 49.5)),  
1:length(crop(worldclim[[1]], extent(3.5, 11.5, 41.5, 49.5))))  
lons <- unique(xy[,1])  
lats <- unique(xy[,2])  
wc_month <- unlist(wc_month)  
680 dim(wc_month) <- c(lat = length(lats), lon = length(lons), month = 12)  
wc_month <- s2dv_cube(data = wc_month, lon = lons, lat = lats,  
Datasets = "WorldClim")  
  
weight <- CST_RFWeights(wc_month, lon = exp$lon, lat = exp$lat, nf = 4)
```

685

Code Step 3.

Finally, the downscaling method is run in step 4 using the corrected forecast, the slope and weights computed in the previous steps. Note that this code requires high memory resources, although the computation can be split by start date and realization if necessary. Figure 6 shows the spatial resolution improvement given by RainFARM for a specific date when applying a refinement factor 4 or 100.

690

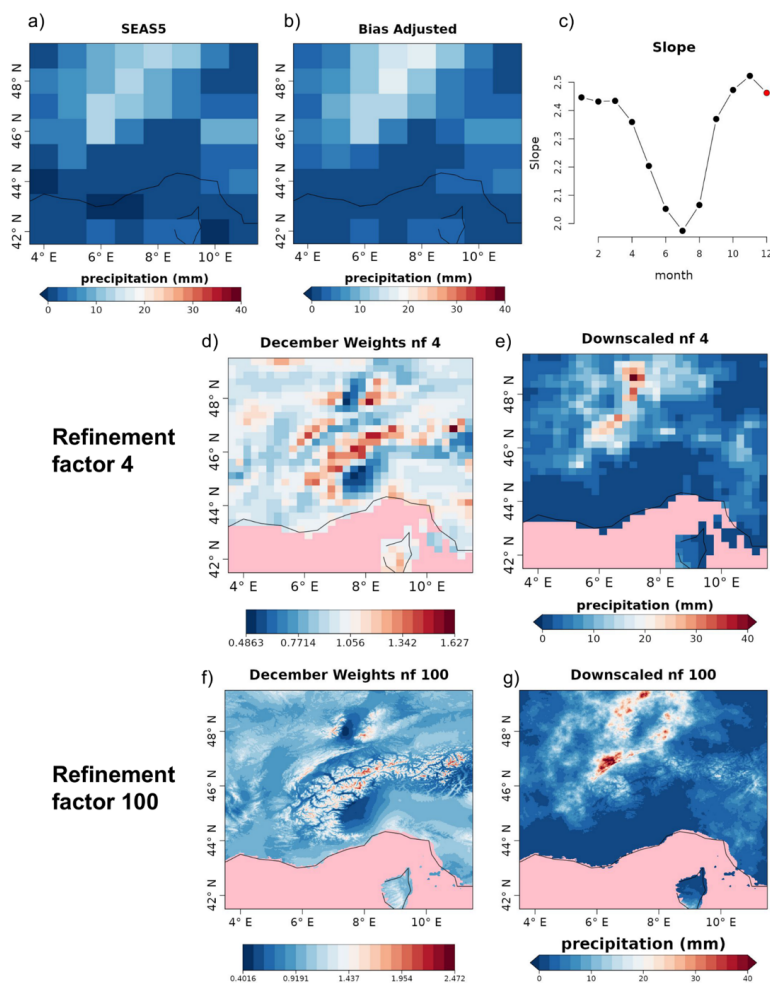
695

700

```
weights <- Subset(weights$data, along = "monthly", indices = c(11,12,1:1:6))  
slope <- Subset(slope, along = "monthly", indices = c(11,12,1:1:6), drop = "non-selected")  
fs <- CST_RainFARM(exp.qm, nf = 4,  
weights = weights, slope = slope,  
kmin = 1, nens = 10, verbose = TRUE,  
time_dim = c("member", "ftime"), nprocs = 4,  
drop_realization = TRUE)  
  
fs <- CST_MergeDims(fs, merge_dims = c("ftime", "monthly"), na.rm = TRUE)  
  
fs$Dates[[1]] <- exp$Dates[[1]]  
CST_SaveExp(fs, destination = "/esarchive/scratch/nperez/CSTools_manuscript")
```

Code Step 4.

705



710 **Figure 6: Original (a) large-scale precipitation field for SEAS5 for the 11th of December 1993 to be downscaled; (b) bias-corrected field; (c) monthly slopes (the slope used for downscaling is highlighted in red). In the middle (refinement factor 4) and bottom (refinement factor 100) rows the comparison of the weights (d and f) and the downscaled (e and g) precipitation fields for SEAS5 for the 11th of December 1993 are shown. Grid points for which no data are available are coloured in pink.**

In addition to total precipitation, the SNOWPACK model requires a number of input variables, namely 2 m air-temperature, atmospheric pressure, relative humidity, shortwave and longwave incoming radiation, wind speed and ground temperature, at finer spatial and temporal resolutions (1 km in space and 1 hour in time) compared to the typical resolutions of the seasonal forecast system outputs (about 100 km in space and 1 day or 6 hours in time). In order to provide the SNOWPACK model with realistic meteorological forcing, we apply bias-adjustment and downscaling techniques depending on the specific variable.

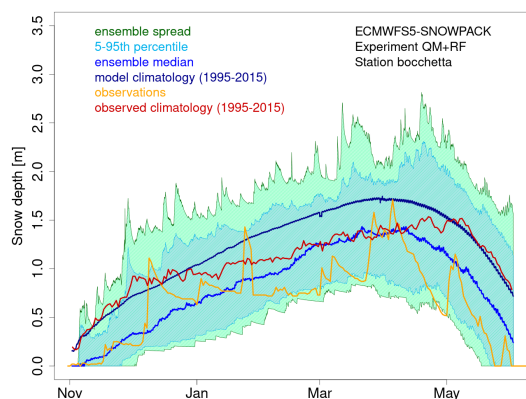
- Seasonal temperature forecasts were bias-corrected using the daily annual climatology of station observations
- All other variables are bilinearly interpolated to the coordinates of the study-sites.

720 After the spatial downscaling, seasonal forecast data are interpolated to one hour temporal resolution with different methods depending on the variable (Terzago et al., in preparation).

Using these high-resolution variables, the SNOWPACK model is run for each of the 21 seasonal forecasts over the hindcast period 1996-2016, considering those initialized on November 1st and covering the 7 months ahead, in order to reproduce the



725 most relevant period for the snow dynamics, i.e. November-May. Figure 7 shows an example of the SNOWPACK model
output, and specifically, the snow depth forecasts obtained from the SEAS5 forecast initialized on the 1st of November 2006,
for the area including the station of Bocchetta delle Pisse —2410 m above sea level (a.s.l.). For each forecast, we obtain an
ensemble of 250 snow depth /SWE simulations, derived from ten downscaling realizations of the precipitation field
produced by 25 ensemble members of the SEAS5 forecast system. SEAS5-SNOWPACK forecasts are able to reproduce the
730 variability of the observed snow depth (Fig. 7). For 2006/2007 in particular, the median forecast is lower than the model
climatology, which is consistent with the low amount of snow that was observed that winter.



735 **Figure 7: Seasonal forecast of snow depth obtained from the SNOWPACK model driven by the SEAS5 seasonal forecast system data. The forecast, initialized on the 1st of November 2006 and covering the 7 following months, refers to the station of Bocchetta delle Pisse, 2410 m a.s.l. in the North-Western Italian Alps. The green shadow shows the spread of the 250 daily snow depth forecast ensemble members; the cyan shadow represents the 5th-95th percentile range of the forecast distribution; the blue line represents the ensemble median of the 250 ensemble members for the 2006/2007 season; the dark blue line represents the model climatology (mean over the seasons 1995-2015 and over all ensemble members); the red line represents the observed climatology and the orange line represents the station observations for the 2006/2007 season.**

740 3.3 Use case 3: Seasonal forecasts for a river flow

In this last use case, we provide downscaled and bias-adjusted seasonal forecasts as input for the hydrological model SCHEME (Baguis et al. 2010), to simulate the river flow of the longest river in Greece, the Aliakmon. This will allow the generation of a seasonal ensemble prediction system that provides the outlooks of water availability for hydro-power and irrigation for the Aliakmon basin (Fig. B1).

745 The SCHEME hydrological model is the semi-distributed version of the daily time-step lumped model developed by Bultot and Dupriez (1976). This model was designed first for the Scheldt and the Meuse River basins in Belgium and Northern France to estimate the impact of climate changes on the hydrological cycle, but it has since been used for hydrological predictions in the seasonal (Roulin and Vannitsem, 2005) and in data assimilation of large-scale satellite soil moisture (Baguis and Roulin, 2017). In addition to daily rainfall, the SCHEME model requires daily minimum, maximum and average
750 temperature as input to calculate the potential evapotranspiration using the Hargreaves and Samani equation (e.g. Oudin et al., 2005). These will be provided for a domain covering the Aliakmon basin and a large part of Greece.

For this use case, post-processing the seasonal forecasts is absolutely necessary as biases must be removed and much higher spatial resolution is necessary. Indeed, while the typical seasonal forecasts are provided at a resolution of around 100 km, the
755 spatial resolution required by the hydrological model is 5 km. Our tailored approach focuses on providing high-quality and high-resolution temperature and precipitation forecasts. An analog approach is used, which combine both the synoptic-scale pressure over Europe and the regional-scale rainfall over Greece. For the best analog day, the high-resolution fields of both



temperature and rainfall over Greece are considered as the end product. This approach ensures the spatio-temporal consistency of both fields. Rather than giving detailed code instructions similar to the previous use cases, an extensive discussion on the data-generation process is provided and the code is made available online. Note again that all steps are being executed using only CSTools functions.

As the reference rainfall dataset, the daily data from CHIRPS (Climate Hazards group Infrared Precipitation with Stations; Funk et al. 2015) is taken, available at 0.05° resolution is used. Moreover, this dataset incorporates corrections for different mountain elevations and slopes, which is necessary in the orographically complex Aliakmon basin with elevations above 2000 m. For temperature, we use the ERA5-Land (Muñoz-Sabater et al., 2021) available at around 0.1° and further downscaled to 0.05° resolution using a simple lapse-rate correction.

Fig. 8 provides the step-by-step structure of the methodology used while Fig. 9 provides a visual representation of the post-processing chain. As shown in Fig. 8, the overall methodology can be separated into a bias adjustment phase (steps 1-2) and a downscaling phase (steps 3-5) that uses an analog approach. The bias adjustment phase starts by loading (using *CST_Load*) the daily forecast and observational rainfall data over Greece at 1° resolution. As forecast data, we take the 25 members of SEAS5 from 1993-2019 initialized in May while the reference is the CHIRPS dataset upscaled to 1° resolution for the same time period. In step 2, these daily rainfall forecasts are bias-adjusted (using *CST_Calibration* with method *bias*) against the CHIRPS dataset. The bias adjustment is done per month of lead time using a leave-one-out or cross-validation approach. Breaking up the data per month was done using the *CST_SplitDim* function.

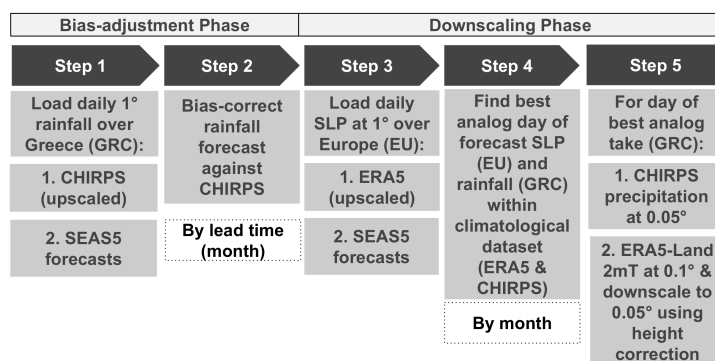
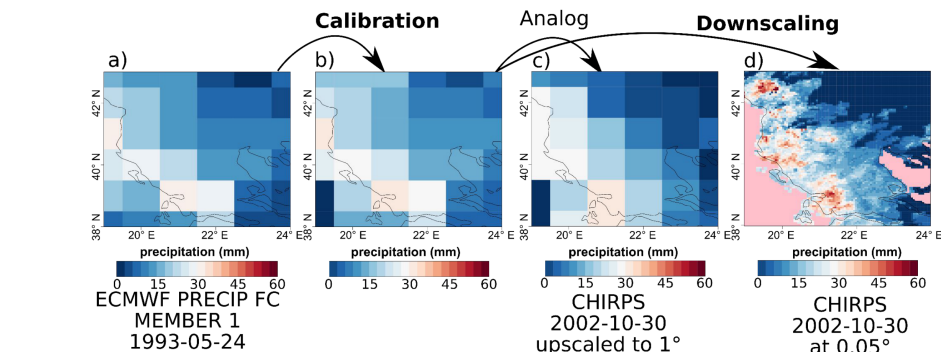


Figure 8: Scheme of the necessary steps to obtain bias adjusted and downscaled input for the hydrological SCHEME model. The abbreviations used are SLP (sea-level pressure), SEAS5, EU (Europe) and GRC (Greece).

The downscaling phase starts in step 3 (see Fig. 8) by loading the sea-level pressure (SLP) of the forecast and reference at 1° resolution over Europe. The reference dataset in this case is ERA5 (Hersbach et al., 2020) and upscaling is applied to obtain the 1° resolution. In step 4, both the bias-adjusted precipitation fields over Greece and the SLP anomaly fields over Europe of a particular forecast day are selected. These fields are then compared to all fields of a large climatological reference dataset in order to find the best analog (using the *Analogs* function). This dataset covers the period 1993-2019 but includes only days with the same month as the selected day (and excludes the selected day). Separating the data per month was again done using the *CST_SplitDim* function. The criterion to find the best analog is called *Local_dist* and minimizes the Euclidean distances of the large-scale SLP and the local-scale rainfall patterns, both at 1° resolution. Finally, for the day corresponding to the best analog, the CHIRPS precipitation field at 0.05° resolution is then considered as the bias-adjusted and downscaled



790 field of the selected day (See Fig. 9c and 9d). In order to obtain the temperature, the ERA5-Land dataset over Greece is considered for the day of the best analog. More specifically, the ERA5-Land daily minimum, maximum and average temperature at 0.1° resolution are downscaled to a resolution of 0.05° using lapse-rate height corrections. Finally, the downscaling procedure steps 4-5 are iterated over all days and all ensemble members of the seasonal forecast in order to obtain a fully bias-corrected and downscaled seasonal forecast over Greece.



795

Figure 9: Comparison of the original forecast (a), bias-adjusted forecast (b), the analog (c) and the downsampled (d) forecast over Greece for SEAS5 for the 24th of May 1993.

4 Conclusions

800 CSTools contains state-of-the-art methods to post-process seasonal forecast datasets specially focusing on statistical correction and downscaling methods, as well as classification methods. These methods are extremely valued in the community given the need of correcting intrinsic systematic model errors and the need of many final applications to have these forecasts in higher resolution than the original resolution provided by the forecast systems. On the other hand, the visualization tools tailored for probabilistic forecasts are able to summarize the results in a concise yet user-friendly manner (see e.g. Fig. 4).

805

Three use cases showcased the ability of the CSTools R package to successfully post-process seasonal forecasts in the context of scientifically advanced impact modelling. The final users potentially interested in these three use cases represent a classical current-day sample of the users (and disciplines) that can benefit from CSTools. The energy sector can see the utility of seasonal forecast post-processed with CSTools in all the use cases presented: the first one showed the potential of seasonal forecasts to anticipate high wind speed events in the Iberian peninsula and the impact it had on energy production and prizes; the second and third cases could be of high interest for the hydrological energy sector since foreseeing months in advance the snow depths at high altitudes and the stream flow in catchments may allow hydropower managers to plan their activity. Similarly, these use cases are relevant for risk management of high wind speed, coastal and flooding events.

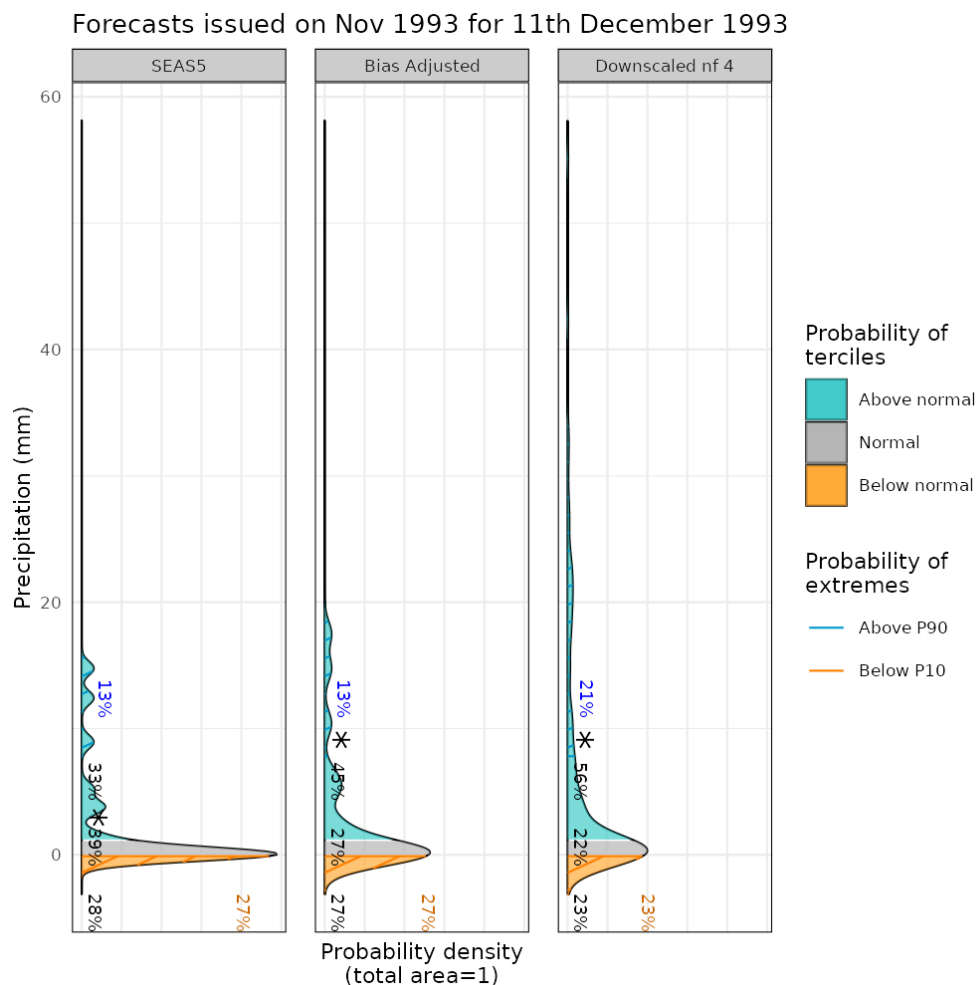
815 Two aspects of the CSTools design are highly valuable: the data loading step in which the user can get the forecast and the reference dataset in a common structure (i.e. the “s2dv_cube” object) simplifying the subsequent data manipulation steps, and the internal use of the multiApply package in the data processing functions making them flexible to work with any number of dimensions and allowing parallel computation.

820 The development guidelines are a fundamental piece of documentation for the future extension of the package when new state-of-the-art methods are required or become available. These guidelines are already being adopted by another R package called CSIndicators that stands for Climate Services Indicators (Pérez-Zanón et. al., 2021), dedicated to calculating the most



suitable tailored indicator for each particular climate service application (agriculture, food security, energy, water management...). Other types of documentation, such as vignettes, provided along with the package, are intended to facilitate the users' learning process.

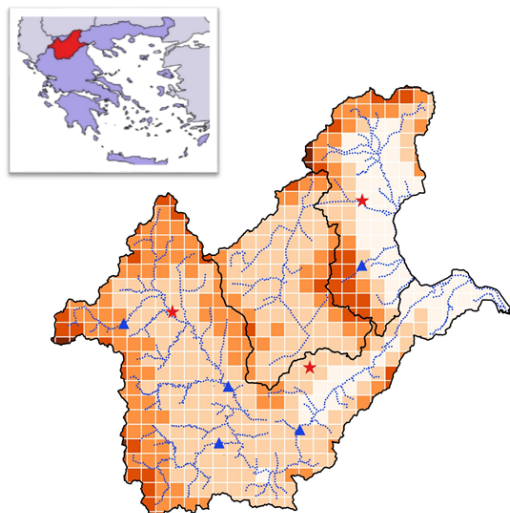
Appendix A: Probabilities distribution use case 2



830 Figure A1: From left to right, PDF for the original, the bias-corrected by quantile mapping and the downscaled precipitation data (for refinement factor 4) SEAS5 for a grid point corresponding to a observational site in the Alps on the 11th of December 1993. For each PDF, three categories of equal size are shown: terciles above normal (blue), normal (grey) and below normal (orange), defined according to the area average of ERA5 reanalysis for the period 1993-2018. Percentages represent the forecast probabilities of each tercile, the most likely tercile is highlighted with a star and the blue and orange percentages represent the probabilities for P10 and P90 (hatched areas), respectively.



Appendix B: Aliakmon river basin



835

Figure B1: Aliakmon river basin and the SCHEME hydrological model: in white: model grid; small blue dots: points at every km along the river; red stars: weather stations; blue triangles: stream gauges; elevation 0 to 2293 m.

Code availability

840

CSTools is released under the Apache License version 2.0. The latest release of CSTools 4.0.1 is publicly available on CRAN repository <https://CRAN.R-project.org/package=CSTools>, it is being developed at BSC-CNS GitLab repository <https://earth.bsc.es/gitlab/external/cstools/> and shared in the Zenodo DOI:[10.5281/zenodo.5549474](https://doi.org/10.5281/zenodo.5549474). The code to reproduce the use cases and plots shown in this manuscript is shared in the three sites and we recommend to find it at the GitLab repository <https://earth.bsc.es/gitlab/external/cstools/-/tree/master/inst/doc>.

845 Author contribution

Núria Pérez-Zanón developed several functions in the package: *CST_SaveExp*, *CST_SplitDims*, *CST_MergeDims*, *CST_QuantileMapping*, *CST_MultiMetric*, *s2dv_cube* and *as.s2dv_cube*. She, as maintainer, also co-managed the package with Louis-Philippe Caron. Silvia Terzago and Bert Van Schaeybroeck together with Emmanuel Roulin designed the second and third use cases presented in the manuscript, respectively. Llorenç Lledó created the function *PlotForecastPDF* and designed the first use case presented in this manuscript. Nicolau Manubens provided advice on the design of the API and compatibility with other packages, drafted the CSTools development guidelines, developed the *CST_Load* and *PlotCombinedMap* functions and created the sample data provided along with the package. Carmen Alvarez-Castro created the *Analogs* function and the dynamical bias correction methodology. Lauriane Batté adapted the ADAMONT downscaling methodology to CSTools. Bert Van Schaeybroeck also developed the *CategoricalEnsCombination* function and the methods bias, *evmos*, and *crps* in *Calibration* function. Verónica Torralba developed the *mse_min* method while Carlos Delgado-Torres added the *rpc*-based method to the *Calibration* function. Marta Domínguez adapted the *AnalogsPredictors* downscaling methodology to be included in CSTools. Jost von Hardenberg developed the RainFARM functionalities, as well as the *RFTemp*, and he adapted *MultiEOFs* and *EnsClustering* functions to CSTools guidelines. Eroteida Sánchez-García coded the BEI methodology and the *PlotPDFsOLE* visualization function. Verónica Torralba also coded the *BiasCorrection*,

850

855



860 *WeatherRegimes*, *RegimesAssign*, *PlotMostLikelyQuantileMaps* and *PlotTriangles4Categories* functions. Deborah Verfaillie created the *CST_MultivarRMSE* function. Núria Pérez-Zanón prepared the manuscript with contributions from all co-authors.

Competing interests. The authors declare that they have no conflict of interest.

865 Acknowledgments

This work has been performed in the framework of the MEDSCOPE (MEDiterranean Services Chain based On climate PrEdictions) ERA4CS project (GA 690462) with contributions from the Sub-seasonal to Seasonal climate forecasting for Energy (S2S4E; GA 776787) and the European Climate Prediction system (EUCP; GA 776613) from the European Union's Horizon 2020 research and innovation programme. CDT acknowledges the funding by the Spanish Ministry for Science and Innovation (FPI PRE2019-088646). We thank other contributors to the CSTools package: Filippo Cali Quaglia, Chihchung Chou, Nicola Cortesi, Susanna Corti, Paolo Davini, Federico Fabiano, Ignazio Giuntol, Raúl Marcos, Niti Mishra, Jesus Peña, Francesc Roura-Adserias and Danila Volpi. We also thank Pierre-Antoine Bretonnière and Margarida Samsó for their support on data formatting, An-Chi Ho for her work on *s2dv*, *s2dverification* and *startR* packages, and Kim Serradell and Francesco Benincasa for the technical support. The R community and especially the developers of the packages *rainfarmr*, *multiApply*, *ClimProjDiags*, *ncdf4*, *plyr*, *abind*, *data.table*, *reshape2*, *ggplot2*, *qmap*, *RColorBrewer*, *verification*, *zeallot*, *testthat*, *knitr*, *markdown* and *rmarkdown* are sincerely acknowledged, as well as the CDO developers.

References

- AEMET: Informe Mensual Climatológico Marzo de 2018. [online] Available from: http://www.aemet.es/documentos/es/serviciosclimaticos/vigilancia_clima/resumenes_climat/mensuales/2018/res_mens_clim_2018_03.pdf (Accessed 25 October 2021), 2018.
- 880 Baguis, P., Roulin, E., Willems, P., and Ntegeka, V.: Climate change and hydrological extremes in Belgian catchments, *Hydrol. Earth Syst. Sci. Discuss.*, 7(4), 5033–5078, doi:10.5194/hessd-7-5033-2010, 2010.
- Baguis, P. and Roulin, E.: Soil moisture data assimilation in a hydrological model: A case study in Belgium using large-scale satellite data, *Remote Sens.*, 9(8), doi:10.3390/rs9080820, 2017.
- 885 Balling, R. C.: Classification in Climatology, in *Spatial Statistics and Models*, 81–108 pp., Springer Netherlands., 1984.
- Bartelt, P. and Lehning, M.: A physical SNOWPACK model for the Swiss avalanche warning Part I: Numerical model, *Cold Reg. Sci. Technol.*, 35(3), 123–145, doi:10.1016/S0165-232X(02)00074-5, 2002.
- Boer, G. J., Smith, D. M., Cassou, C., Doblas-Reyes, F., Danabasoglu, G., Kirtman, B., Kushnir, Y., Kimoto, M., Meehl, G. A., Msadek, R., Mueller, W. A., Taylor, K. E., Zwiers, F., Rixen, M., Ruprich-Robert, Y., and Eade, R.: The Decadal Climate Prediction Project (DCPP) contribution to CMIP6, *Geosci. Model Dev.*, 9(10), 3751–3777, doi:10.5194/gmd-9-3751-2016, 2016.
- 890 BSC-CNS and Manubens, N.: *startR*: Automatically Retrieve Multidimensional Distributed Data Sets, [online] Available from: <https://cran.r-project.org/package=startR>, 2020.
- BSC-CNS, Manubens, N., and Hunter, A.: *Apply Functions to Multiple Multidimensional Arrays or Vectors*, [online] Available from: <https://cran.r-project.org/package=multiApply>, 2019.
- 895 Brady, R. X. and Spring, A.: *climpred*: Verification of weather and climate forecasts, *J. Open Source Softw.*, 6(59), 2781, doi:10.21105/JOSS.02781, 2021.
- Bultot, F. and Dupriez, G. L.: Conceptual hydrological model for an average-sized catchment area, I. Concepts and relationships, *J. Hydrol.*, 29(3–4), 251–272, doi:10.1016/0022-1694(76)90040-8, 1976.



- 900 Chacon, S. and Straub, B.: Pro git. Apress, 2014.
Cortesi, N., Torralba, V., González-Reviriego, N., Soret, A., and Doblas-Reyes, F. J.: Characterization of European wind speed variability using weather regimes, *Clim. Dyn.*, 53(7–8), 4961–4976, doi:10.1007/s00382-019-04839-5, 2019.
D’Onofrio, D., Palazzi, E., Von Hardenberg, J., Provenzale, A., and Calmanti, S.: Stochastic rainfall downscaling of climate models, *J. Hydrometeorol.*, 15(2), 830–843, doi:10.1175/JHM-D-13-096.1, 2014.
- 905 Doblas-Reyes, F. J., Hagedorn, R., and Palmer, T. N.: The rationale behind the success of multi-model ensembles in seasonal forecasting - II. Calibration and combination, *Tellus A*, 57(3), 234–252, doi:10.1111/j.1600-0870.2005.00104.x, 2005.
Drechsel, S., Mayr, G. J., Messner, J. W., and Stauffer, R.: Wind speeds at heights crucial for wind energy: Measurements and verification of forecasts, *J. Appl. Meteorol. Climatol.*, 51(9), 1602–1617, doi:10.1175/JAMC-D-11-0247.1, 2012.
- 910 Eade, R., Smith, D., Scaife, A., Wallace, E., Dunstone, N., Hermanson, L., and Robinson, N.: Do seasonal-to-decadal climate predictions underestimate the predictability of the real world?, *Geophys. Res. Lett.*, 41(15), 5620–5628, doi:10.1002/2014GL061146, 2014.
ECMWF: SEAS5 user guide, 43 pp. [online] Available from: https://www.ecmwf.int/sites/default/files/medialibrary/2017-10/System5_guide.pdf (Accessed 22 October 2020), 2017.
- 915 Eyring, V., Bock, L., Lauer, A., Righi, M., Schlund, M., Andela, B., Arnone, E., Bellprat, O., Brötz, B., Caron, L.P., Carvalho, N., Cionni, I., Cortesi, N., Crezee, B., L. Davin, E., Davini, P., Debeire, K., De Mora, L., Deser, C., Docquier, D., Earnshaw, P., Ehbrecht, C., K. Gier, B., Gonzalez-Reviriego, N., Goodman, P., Hagemann, S., Hardiman, S., Hassler, B., Hunter, A., Kadow, C., Kindermann, S., Koirala, S., Koldunov, N., Lejeune, Q., Lembo, V., Lovato, T., Lucarini, V., Massonnet, F., Müller, B., Pandde, A., Pérez-Zanón, N., Phillips, A., Predoi, V., Russell, J., Sellar, A., Serva, F., Stacke, T.,
- 920 Swaminathan, R., Torralba, V., Vegas-Regidor, J., Von Hardenberg, J., Weigel, K., and Zimmermann, K.: Earth System Model Evaluation Tool (ESMValTool) v2.0 - An extended set of large-scale diagnostics for quasi-operational and comprehensive evaluation of Earth system models in CMIP, *Geosci. Model Dev.*, 13(7), 3383–3438, doi:10.5194/gmd-13-3383-2020, 2020.
Eyring, V., Bony, S., Meehl, G. A., Senior, C. A., Stevens, B., Stouffer, R. J., and Taylor, K. E.: Overview of the Coupled
925 Model Intercomparison Project Phase 6 (CMIP6) experimental design and organization, *Geosci. Model Dev.*, 9(5), 1937–1958, doi:10.5194/gmd-9-1937-2016, 2016a.
Eyring, V., Righi, M., Lauer, A., Evaldsson, M., Wenzel, S., Jones, C., Anav, A., Andrews, O., Cionni, I., Davin, E. L., Deser, C., Ehbrecht, C., Friedlingstein, P., Gleckler, P., Gottschaldt, K.-D., Hagemann, S., Juckes, M., Kindermann, S., Krasting, J., Kunert, D., Levine, R., Loew, A., Mäkelä, J., Martin, G., Mason, E., Phillips, A. S., Read, S., Rio, C., Roehrig,
- 930 R., Senftleben, D., Sterl, A., van Ulft, L. H., Walton, J., Wang, S., and Williams, K. D.: ESMValTool (v1.0) – a community diagnostic and performance metrics tool for routine evaluation of Earth system models in CMIP, *Geosci. Model Dev.*, 9(5), 1747–1802, doi:10.5194/gmd-9-1747-2016, 2016b.
Faranda, D., Alvarez-Castro, M. C., Messori, G., Rodrigues, D., and Yiou, P.: The hammam effect or how a warm ocean enhances large scale atmospheric predictability, *Nat. Commun.*, 10(1), 1–7, doi:10.1038/s41467-019-09305-8, 2019.
- 935 Faranda, D., Messori, G., and Yiou, P.: Dynamical proxies of North Atlantic predictability and extremes, *Sci. Rep.*, 7(1), 1–10, doi:10.1038/srep41278, 2017.
Ferranti, L. and Corti, S.: New clustering products., *ECMWF Newsl.*, 127(1–2), 6–11, doi:10.21957/lr3bcise, 2011.
Fick, S. E. and Hijmans, R. J.: WorldClim 2: new 1-km spatial resolution climate surfaces for global land areas, *Int. J. Climatol.*, 37(12), 4302–4315, doi:10.1002/joc.5086, 2017.
- 940 Funk, C., Peterson, P., Landsfeld, M., Pedreros, D., Verdin, J., Shukla, S., Husak, G., Rowland, J., Harrison, L., Hoell, A., and Michaelsen, J.: The climate hazards infrared precipitation with stations - A new environmental record for monitoring extremes, *Sci. Data*, 2(1), 1–21, doi:10.1038/sdata.2015.66, 2015.



- Gudmundsson, L., Bremnes, J. B., Haugen, J. E., and Engen-Skaugen, T.: Technical Note: Downscaling RCM precipitation to the station scale using statistical transformations – a comparison of methods, *Hydrol. Earth Syst. Sci.*, 16(9), 3383–3390, doi:10.5194/hess-16-3383-2012, 2012.
- 945 Gudmundsson, L.: qmap: Statistical Transformations for Post-Processing Climate Model Output, CRAN [online] Available from: <https://cran.r-project.org/package=qmap>, 2016.
- Hagedorn, R., Doblas-Reyes, F. J., and Palmer, T. N.: The rationale behind the success of multi-model ensembles in seasonal forecasting-I. Basic concept, *Tellus A Dyn. Meteorol. Oceanogr.*, 57, 219–233, doi:10.3402/tellusa.v57i3.14657, 950 2005.
- Hemri, S., Bhend, J., Liniger, M. A., Manzanas, R., Siegert, S., Stephenson, D. B., Gutiérrez, J. M., Brookshaw, A., and Doblas-Reyes, F. J.: How to create an operational multi-model of seasonal forecasts?, *Clim. Dyn.*, 55(5–6), 1141–1157, doi:10.1007/s00382-020-05314-2, 2020.
- Hersbach, H., Bell, B., Berrisford, P., Hirahara, S., Horányi, A., Muñoz-Sabater, J., Nicolas, J., Peubey, C., Radu, R., 955 Schepers, D., Simmons, A., Soci, C., Abdalla, S., Abellan, X., Balsamo, G., Bechtold, P., Biavati, G., Bidlot, J., Bonavita, M., De Chiara, G., Dahlgren, P., Dee, D., Diamantakis, M., Dragani, R., Flemming, J., Forbes, R., Fuentes, M., Geer, A., Haimberger, L., Healy, S., Hogan, R. J., Hólm, E., Janisková, M., Keeley, S., Laloyaux, P., Lopez, P., Lupu, C., Radnoti, G., de Rosnay, P., Rozum, I., Vamborg, F., Villaume, S., and Thépaut, J. N.: The ERA5 global reanalysis, *Q. J. R. Meteorol. Soc.*, 146(730), 1999–2049, doi:10.1002/qj.3803, 2020.
- 960 Hijmans, R. J.: raster: Geographic Data Analysis and Modeling, CRAN [online] Available from: <https://cran.r-project.org/package=raster>, 2020.
- Information Resources Management Association: *Software Design and Development: Concepts, Methodologies, Tools, and Applications*, edited by IGI Global, USA, 2013.
- Iturbide, M., Bedia, J., Herrera, S., Baño-Medina, J., Fernández, J., Frías, M. D., Manzanas, R., San-Martín, D., Cimadevilla, 965 E., Cofiño, A. S. and Gutiérrez, J. M.: The R-based climate4R open framework for reproducible climate data access and post-processing, *Environ. Model. Softw.*, 111, 42–54, doi:10.1016/J.ENVSOF.2018.09.009, 2019.
- Kirtman, B. P., Min, D., Infanti, J. M., Kinter, J. L., Paolino, D. A., Zhang, Q., Van Den Dool, H., Saha, S., Mendez, M. P., Becker, E., Peng, P., Tripp, P., Huang, J., Dewitt, D. G., Tippet, M. K., Barnston, A. G., Li, S., Rosati, A., Schubert, S. D., Rienecker, M., Suarez, M., Li, Z. E., Marshak, J., Lim, Y. K., Tribbia, J., Pegion, K., Merryfield, W. J., Denis, B., and 970 Wood, E. F.: The North American multimodel ensemble: Phase-1 seasonal-to-interannual prediction; phase-2 toward developing intraseasonal prediction, *Bull. Am. Meteorol. Soc.*, 95(4), 585–601, doi:10.1175/BAMS-D-12-00050.1, 2014.
- Lehning, M., Bartelt, P., Brown, B., and Fierz, C.: A physical SNOWPACK model for the Swiss avalanche warning Part III: Meteorological forcing, thin layer formation and evaluation, *Cold Reg. Sci. Technol.*, 35(3), 169–184, doi:10.1016/S0165-232X(02)00072-1, 2002a.
- 975 Lehning, M., Bartelt, P., Brown, B., Fierz, C., and Satyawali, P.: A physical SNOWPACK model for the Swiss avalanche warning Part II. Snow microstructure, *Cold Reg. Sci. Technol.*, 35(3), 147–167, doi:10.1016/S0165-232X(02)00073-3, 2002b.
- Lledó, L., Cionni, I., Torralba, V., Bretonnière, P.A., and Samsó, M.: Seasonal prediction of Euro-Atlantic teleconnections from multiple systems, *Environ. Res. Lett.*, 15(7), 074009, doi:10.1088/1748-9326/ab87d2, 2020a.
- 980 Lledó, L. and Doblas-Reyes, F. J.: Predicting daily mean wind speed in Europe weeks ahead from MJO status, *Mon. Weather Rev.*, doi:10.1175/mwr-d-19-0328.1, 2020b.
- Manubens, N., Caron, L.-P., Hunter, A., Bellprat, O., Exarchou, E., Fuckar, N. S., Garcia-Serrano, J., Massonnet, F., En Egoz, M. M., Sicardi, V., Batt E C, Chlo E Prodhomme, L., Onica Torralba, V., Cortesi, N., Mula-Valls, O., Serradell, K., Guemas, V., and Doblas-Reyes, F. J.: An R package for climate forecast verification, *Environ. Model. Softw.*, 103, 29–42, 985 doi:10.1016/j.envsoft.2018.01.018, 2018.



- Manzanas, R., Gutiérrez, J. M., Bhend, J., Hemri, S., Doblas-Reyes, F. J., Torralba, V., Penabad, E., and Brookshaw, A.: Bias adjustment and ensemble recalibration methods for seasonal forecasting: a comprehensive intercomparison using the C3S dataset, *Clim. Dyn.*, 53(3–4), 1287–1305, doi:10.1007/s00382-019-04640-4, 2019.
- Maraun, D., Wetterhall, F., Ireson, A. M., Chandler, R. E., Kendon, E. J., Widmann, M., Brienen, S., Rust, H. W., Sauter, T.,
990 Themel, M., Venema, V. K. C., Chun, K. P., Goodess, C. M., Jones, R. G., Onof, C., Vrac, M., and Thiele-Eich, I.: Precipitation downscaling under climate change: Recent developments to bridge the gap between dynamical models and the end user, *Rev. Geophys.*, 48(3), RG3003, doi:10.1029/2009RG000314, 2010.
- Maraun, D. and Widmann, M.: *Statistical Downscaling and Bias Correction for Climate Research*, Cambridge University Press, 2018.
- 995 Marcos, R.: Improvement of seasonal forecasting techniques applied to water resources and forest fires, Universitat de Barcelona. [online] Available from: www.tdx.cat (Accessed 1 October 2020), 2016.
- Merryfield, W. J., Baehr, J., Batté, L., Becker, E. J., Butler, A. H., Coelho, C. A. S., Danabasoglu, G., Dirmeyer, P. A., Doblas-Reyes, F. J., Domeisen, D. I. V., Ferranti, L., Ilynia, T., Kumar, A., Müller, W. A., Rixen, M., Robertson, A. W., Smith, D. M., Takaya, Y., Tuma, M., Vitart, F., White, C. J., Alvarez, M. S., Ardilouze, C., Attard, H., Baggett, C.,
1000 Balmaseda, M. A., Beraki, A. F., Bhattacharjee, P. S., Bilbao, R., De Andrade, F. M., DeFlorio, M. J., Díaz, L. B., Ehsan, M. A., Fragkoulidis, G., Grainger, S., Green, B. W., Hell, M. C., Infanti, J. M., Isensee, K., Kataoka, T., Kirtman, B. P., Klingaman, N. P., Lee, J. Y., Mayer, K., McKay, R., Mecking, J. V., Miller, D. E., Neddermann, N., Ng, C. H. J., Ossó, A., Pankatz, K., Peatman, S., Pegion, K., Perlwitz, J., Recalde-Coronel, G. C., Reintges, A., Renkl, C., Solaraju-Murali, B., Spring, A., Stan, C., Sun, Y. Q., Tozer, C. R., Vigaud, N., Woolnough, S., and Yeager, S.: Current and emerging
1005 developments in subseasonal to decadal prediction, *Bull. Am. Meteorol. Soc.*, 101(6), E869–E896, doi:10.1175/BAMS-D-19-0037.1, 2020.
- MeteoSwiss: easyVerification: Ensemble Forecast Verification for Large Data Sets, CRAN [online] Available from: <https://cran.r-project.org/package=easyVerification>, 2017.
- Min, Y. M., Kryjov, V. N., and Oh, S. M.: Assessment of APCC multimodel ensemble prediction in seasonal climate
1010 forecasting: Retrospective (1983–2003) and real-time forecasts (2008–2013), *J. Geophys. Res.*, 119(21), 12,132–12,150, doi:10.1002/2014JD022230, 2014.
- Mishra, N., Prodhomme, C., and Guemas, V.: Multi-Model Skill Assessment of Seasonal Temperature and Precipitation Forecasts over Europe, *Clim. Dyn.*, 52(7–8), 4207–4225, doi:https://doi.org/10.1007/s00382-018-4404-z, 2019.
- Muñoz-Sabater, J., Dutra, E., Agustí-Panareda, A., Albergel, C., Arduini, G., Balsamo, G., Boussetta, S., Choulga, M.,
1015 Harrigan, S., Hersbach, H., Martens, B., Miralles, D., Piles, M., Rodríguez-Fernández, N., Zsoter, E., Buontempo, C., and Thépaut, J.N.: ERA5-Land: A state-of-the-art global reanalysis dataset for land applications, *Earth Syst. Sci. Data Discuss.*, 1–50, doi:10.5194/essd-2021-82, 2021.
- National Academies of Sciences, Engineering and Medicine: *Next Generation Earth System Prediction: Strategies for Subseasonal to Seasonal Forecasts*, Natl. Acad. Press, doi:10.17226/21873, 2016.
- 1020 Oudin, L., Hervieu, F., Michel, C., Perrin, C., Andréassian, V., Anctil, F., and Loumagne, C.: Which potential evapotranspiration input for a lumped rainfall-runoff model? Part 2 - Towards a simple and efficient potential evapotranspiration model for rainfall-runoff modelling, *J. Hydrol.*, 303(1–4), 290–306, doi:10.1016/j.jhydrol.2004.08.026, 2005.
- Palmer, T. N., Doblas-Reyes, F. J., Weisheimer, A., and Rodwell, M. J.: Toward seamless prediction: Calibration of climate
1025 change projections using seasonal forecasts, *Bull. Am. Meteorol. Soc.*, 89(4), 459–470, doi:10.1175/BAMS-89-4-459, 2008.
- Peral García, C., Navascués Fernández-Victorio, B., and Ramos Calzado, P. (2017). Serie de precipitación diaria en rejilla con fines climáticos. Nota Técnica 24 de AEMET. Retrieved from



- https://www.aemet.es/documentos/es/conocerlas/recursos_en_linea/publicaciones_y_estudios/publicaciones/NT_24_AEM ET/NT_24_AEMET.pdf
- 1030 Pérez-Zanón, N., Chihchung, C., and Lledó, L.: CSIndicators: Sectoral Indicators for Climate Services Based on Sub-Seasonal to Decadal Climate Predictions, CRAN [online] Available from: <https://cran.r-project.org/package=CSIndicators>, 2021.
- Pierce, D.: ncd4: Interface to Unidata netCDF (Version 4 or Earlier) Format Data Files, CRAN [online] Available from: <https://CRAN.R-project.org/package=ncdf4>, 2019.
- 1035 R Core Team: R: A language and environment for statistical computing, R Found. Stat. Comput., 2017.
- Rajagopalan, B., Lall, U., and Zebiak, S. E.: Categorical climate forecasts through regularization and optimal combination of multiple GCM ensembles, *Mon. Weather Rev.*, 130(7), 1792–1811, doi:10.1175/1520-0493(2002)130<1792:CCFTRA>2.0.CO;2, 2002.
- Ramon, J., Lledó, L., Bretonniere, P. A., Samsó, M., and Doblas-Reyes, F. J.: A perfect prognosis downscaling methodology for seasonal prediction of local-scale wind speeds, *Environ. Res. Lett.*, 16(5), 54010, doi:10.1088/1748-9326/abe491, 2021.
- 1040 Reborá, N., Ferraris, L., von Hardenberg, J., and Provenzale, A.: Rainfall downscaling and flood forecasting: a case study in the Mediterranean area, *Nat. Hazards Earth Syst. Sci.*, 6(4), 611–619, doi:10.5194/nhess-6-611-2006, 2006a.
- Reborá, N., Ferraris, L., von Hardenberg, J., and Provenzale, A.: RainFARM: Rainfall downscaling by a Filtered Autoregressive Model, *J. Hydrometeorol.*, 7(4), 724–738, doi:10.1175/JHM517.1, 2006b.
- 1045 Red Eléctrica de España: Informe del Sistema Eléctrico Español 2018, [online] Available from: https://www.ree.es/sites/default/files/11_PUBLICACIONES/Documentos/InformesSistemaElectrico/2018/inf_sis_elec_ree_2018.pdf (Accessed 7 June 2021), 2018.
- Righi, M., Andela, B., Eyring, V., Lauer, A., Predoi, V., Schlund, M., Vegas-Regidor, J., Bock, L., Brötz, B., de Mora, L., Diblen, F., Dreyer, L., Drost, N., Earnshaw, P., Hassler, B., Koldunov, N., Little, B., Loosveldt Tomas, S., and Zimmermann, K.: Earth System Model Evaluation Tool (ESMValTool) v2.0 – technical overview, *Geosci. Model Dev.*, 13(3), 1179–1199, doi:10.5194/gmd-13-1179-2020, 2020.
- 1050 Robertson, A. W., Lall, U., Zebiak, S. E., and Goddard, L.: Improved combination of multiple atmospheric GCM ensembles for seasonal prediction, *Mon. Weather Rev.*, 132(12), 2732–2744, doi:10.1175/MWR2818.1, 2004.
- Rössler, O., Fischer, A. M., Huebener, H., Maraun, D., Benestad, R. E., Christodoulides, P., Soares, P. M. M., Cardoso, R. M., Pagé, C., Kanamaru, H., Kreienkamp, F., and Vlachogiannis, D.: Challenges to link climate change data provision and user needs: Perspective from the COST-action VALUE, *Int. J. Climatol.*, 39(9), 3704–3716, doi:10.1002/joc.5060, 2019.
- 1055 Roulin, E. and Vannitsem, S.: Skill of medium-range hydrological ensemble predictions, *J. Hydrometeorol.*, 6(5), 729–744, doi:10.1175/JHM436.1, 2005.
- Sánchez-García, E., Voces-Aboy, J., Navascués, B., and Rodríguez-Camino, E.: Regionally improved seasonal forecast of precipitation through Best estimation of winter NAO, *Adv. Sci. Res.*, 16, 165–174, doi:10.5194/asr-16-165-2019, 2019.
- 1060 Siegert, S.: SpecsVerification: Forecast Verification Routines for Ensemble Forecasts of Weather and Climate, CRAN [online] Available from: <https://cran.r-project.org/package=SpecsVerification>, 2017.
- Sokal, R. R.: Numerical Taxonomy, *Sci. Am.*, 215(6), 106–116, doi:10.1038/scientificamerican1266-106, 1966.
- Soret, A., Torralba, V., Cortesi, N., Christel, I., Palma, L., Manrique-Suñén, A., Lledó, L., González-Reviriego, N., and Doblas-Reyes, F. J.: Sub-seasonal to seasonal climate predictions for wind energy forecasting, in *Journal of Physics: Conference Series*, vol. 1222, 012009, Institute of Physics Publishing., 2019.
- 1065 Schulzweida, U.: CDO User Guide (Version 1.9.8), doi:<http://doi.org/10.5281/zenodo.3539275>, 2019.
- Teetor, N.: Multiple, Unpacking, and Deconstructing Assignment, CRAN [online] Available from: <https://cran.r-project.org/package=zeallot> (Accessed 18 September 2020), 2018.
- 1070 Terzago, S., Bongiovanni, G., and von Hardenberg, J.: Seasonal forecasting of snow resources at Alpine sites, in preparation.



- Terzago, S., Bongiovanni, G., and von Hardenberg, J.: High quality climate prediction, *Medcpe Proj.*, 29 pp., [online] Available from: <https://drive.google.com/file/d/1qp2gbtKdBI4XmsyOeaEhFENwpeUuJwkwf/view> (Accessed 23 November 2020), 2020.
- 1075 Terzago, S., Palazzi, E., and von Hardenberg, J.: Stochastic downscaling of precipitation in complex orography: a simple method to reproduce a realistic fine-scale climatology, *Nat. Hazards Earth Syst. Sci.*, 18(11), 2825–2840, doi:10.5194/nhess-18-2825-2018, 2018.
- Torralba, V.: Seasonal climate prediction for the wind energy sector: methods and tools for the development of a climate service, Universidad Complutense de Madrid. [online] Available from: <https://eprints.ucm.es/56841>, 2019.
- 1080 Torralba, V., Doblas-Reyes, F. J., MacLeod, D., Christel, I., and Davis, M.: Seasonal climate prediction: A new source of information for the management of wind energy resources, *J. Appl. Meteorol. Climatol.*, 56(5), 1231–1247, doi:10.1175/JAMC-D-16-0204.1, 2017.
- Torralba, V., Gonzalez-Reviriego, N., Cortesi, N., Manrique-Suñén, A., Lledó, L., Marcos, R., Soret, A., and Doblas-Reyes, F. J.: Challenges in the selection of atmospheric circulation patterns for the wind energy sector, *Int. J. Climatol.*, 41(3), 1525–1541, doi:10.1002/joc.6881, 2021.
- 1085 Troccoli, A., Harrison, M., Coughlan, M. and Williams, J. B.: Seasonal Forecasts in Decision Making, *Seas. Clim. Forecast. Manag. Risk*, 13–41, doi:10.1007/978-1-4020-6992-5_2, 2008.
- Van Schaeybroeck, B. and Vannitsem, S.: Post-processing through linear regression, *Nonlinear Process. Geophys.*, 18(2), 147–160, doi:10.5194/npg-18-147-2011, 2011.
- 1090 Van Schaeybroeck, B. and Vannitsem, S.: Ensemble post-processing using member-by-member approaches: theoretical aspects, *Q. J. R. Meteorol. Soc.*, 141(688), 807–818, doi:10.1002/qj.2397, 2015.
- Van Schaeybroeck, B. and Vannitsem, S.: Postprocessing of Long-Range Forecasts. In *Statistical Postprocessing of Ensemble Forecasts*, in *Statistical Postprocessing of Ensemble Forecasts*, 267–290, 2019.
- Verfaillie, D., Déqué, M., Morin, S., and Lafaysse, M.: The method ADAMONT v1.0 for statistical adjustment of climate projections applicable to energy balance land surface models, *Geosci. Model Dev.*, 10(11), 4257–4283, doi:10.5194/gmd-10-4257-2017, 2017.
- 1095 Verfaillie, D., Doblas-Reyes, F. J., Donat, M. G., Pérez-Zanón, N., Solaraju-Murali, B., Torralba, V., and Wild, S.: How reliable are decadal climate predictions of near-surface air temperature?, *J. Clim.*, 34(2), 697–713, doi:10.1175/JCLI-D-20-0138.1, 2021.
- 1100 Vitart, F., Huddleston, M. R., Déqué, M., Peake, D., Palmer, T. N., Stockdale, T. N., Davey, M. K., Ineson, S., and Weisheimer, A.: Dynamically-based seasonal forecasts of Atlantic tropical storm activity issued in June by EUROSIP, *Geophys. Res. Lett.*, 34(16), doi:10.1029/2007GL030740, 2007.
- Wang, B., Lee, J. Y., Kang, I. S., Shukla, J., Park, C. K., Kumar, A., Schemm, J., Cocke, S., Kug, J. S., Luo, J. J., Zhou, T., Wang, B., Fu, X., Yun, W. T., Alves, O., Jin, E. K., Kinter, J., Kirtman, B., Krishnamurti, T., Lau, N. C., Lau, W., Liu, P., Pegion, P., Rosati, T., Schubert, S., Stern, W., Suarez, M., and Yamagata, T.: Advance and prospectus of seasonal prediction: Assessment of the APCC/ CliPAS 14-model ensemble retrospective seasonal prediction (1980-2004), *Clim. Dyn.*, 33(1), 93–117, doi:10.1007/s00382-008-0460-0, 2009.
- 1105 White, C. J., Carlsen, H., Robertson, A. W., Klein, R. J. T., Lazo, J. K., Kumar, A., Vitart, F., Coughlan de Perez, E., Ray, A. J., Murray, V., Bharwani, S., MacLeod, D., James, R., Fleming, L., Morse, A. P., Eggen, B., Graham, R., Kjellström, E., Becker, E., Pegion, K. V., Holbrook, N. J., McEvoy, D., Depledge, M., Perkins-Kirkpatrick, S., Brown, T. J., Street, R., Jones, L., Remenyi, T. A., Hodgson-Johnston, I., Buontempo, C., Lamb, R., Meinke, H., Arheimer, B., and Zebiak, S. E.: Potential applications of subseasonal-to-seasonal (S2S) predictions, *Meteorol. Appl.*, 24(3), 315–325, doi:10.1002/met.1654, 2017.



Yiou, P., Salameh, T., Drobinski, P., Menut, L., Vautard, R., and Vrac, M.: Ensemble reconstruction of the atmospheric column from surface pressure using analogues, *Clim. Dyn.*, 41(5–6), 1333–1344, doi:10.1007/s00382-012-1626-3, 2013.

1115